Abstract

Thermodynamic Investigation into Copper Binding in the N-Terminal Region of the Prion Protein at Low Copper Loadings

By

Devi Praneetha Gogineni

December 2010

Chair: Rickey Hicks, Ph.D.

Major Department: Chemistry

The prion protein (PrP) is a naturally occurring protein found at high levels in central nervous system (CNS). The misfolding of the PrP is responsible for neurodegenerative diseases called transmissible spongioform encephalopathies (TSE) that include mad cow disease, scrapie in sheep and goats, kuru and Creutzfelt-Jakob disease (CJD) in humans. The normal function of the PrP is still unknown but demonstrates high selectivity for copper (Cu^{+2}). The mature form of PrP consists of a highly unstructured N-terminal region (23-124). The copper binding region spans from residues 60 to 96 and contains four octarepeat segments, PHGGGWGQ, and a GGGTH segment. When fully copper loaded, each octarepeat binds to a copper and the fifth copper binding involves the GGGTH site. Although the molecular details of a fully Cu^{+2} loaded state are well understood, very little is known about the low copper binding state of PrP. At low Cu^{+2}occupancy there is a possibility of PrP cross-linking. This project aims at obtaining the thermodynamic profile of the prion copper complex at low copper loading state to determine the forces that drive the complex formation. The model peptides were generated using solid phase

peptide synthesis; the thermodynamic studies were done using isothermal titration calorimetry (ITC) and supporting spectroscopic studies by circular dichroism (CD). Examination of the ITC titration data suggests an initial binding event where two PrP's are cross-linked by a single copper ion. ITC titrations were performed in both forward and reverse directions in order to examine the reversibility of the copper binding process. Fitting the ITC data with the existing models, i.e one sets of sites, two sets of sites or sequential binding, lead to unsatisfactory fits suggesting a more complex binding process. The hypothesized binding model will hopefully lead to good fits for the ITC data and will support the hypothesis that Cu^{+2} is cross- linking PrP molecules at low equivalents of added Cu^{+2} .

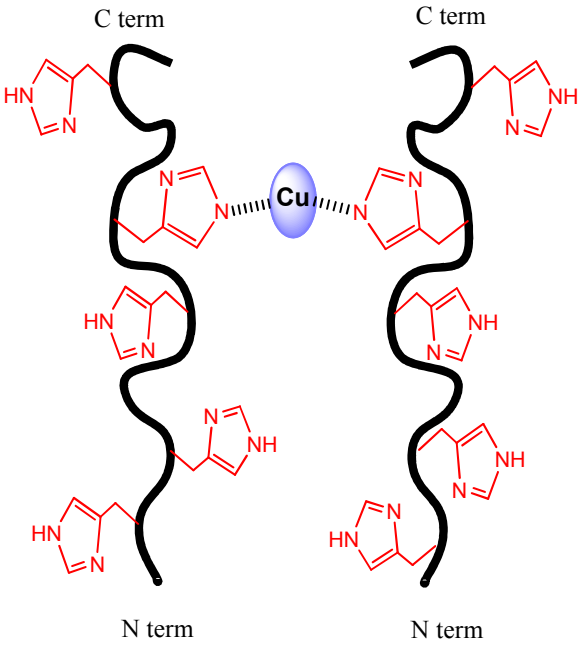

Figure representing the PrP cross linking at low copper loadings

Thermodynamic Investigation into Copper Binding in the N-Terminal Region of the Prion Protein at Low Copper Loadings

A Thesis

Presented To

the Faculty of the Department of Chemistry

East Carolina University

Greenville, NC

In Partial Fulfillment

of the Requirements for the Degree

Masters of Science in Chemistry

By

Devi Praneetha Gogineni

December 2010

Thermodynamic Investigation into Copper Binding

in the N-Terminal Region of the Prion Protein at Low Copper Loadings

By

Devi Praneetha Gogineni

APPROVED BY:

DIRECTOR OF THESIS:_____
Colin S. Burns, Ph.D.

COMMITTEE MEMBER:_____
Anne M. Spuches, Ph.D.

COMMITTEE MEMBER:_____
Art A. Rodriguez, Ph.D.

COMMITTEE MEMBER:_____
William E. Allen, Ph.D.

COMMITTEE MEMBER:_____
Martin Bier, Ph.D.

CHAIR OF THE DEPARTMENT OF CHEMISTRY:_____
Rickey P. Hicks, Ph.D.

DEAN OF THE GRADUATE SCHOOL:_____
Paul J. Gemperline, Ph.D.

Acknowledgements and Dedication

I am very fortunate to pursue my research under the direction of Dr. Colin Burns. I am very thankful to him for his guidance throughout the course of my graduate studies. There were times when I was really amazed by his patience and his passion for research. These two years have been a learning experience giving me a chance to explore and improve myself both professionally and personally. I sincerely thank all the professors and students at ECU who have made it my second home. I am grateful to the department of chemistry, especially Dr. Art Rodriguez for giving me the opportunity to study at ECU. I would like to thank Dr. Anne Spuches for assistance with all the ITC studies. She has been a constant support and her knowledge in chemistry helped me a lot in my research. I also thank Dr. Martin Bier for his suggestions regarding the ITC models.

I would like to dedicate my thesis to my mom, Padmaja Gogineni and my dad, Madana Mohan Rao Gogineni. Their love, support and the moral values they imbibed in me made me the person that I am today. If it wasn't for my dearest sister Haritha Avuthu and my brother in law Pruthvi Avuthu my stay in United States wouldn't have been possible. I thank them for being there for me through thick and thin. I thank my grandparents for keeping me in their prayers. I thank God for giving me such a loving and caring family. I would like to thank my best friends for life Manasa Gangula, Prabha Gade, Sindhuri Maddineni and Aamani Murari for putting up with me for the past 7 years and being the closest people to my heart. I cannot forget the day I and Ramya Garapati joined Dr. Burns lab or the conversations we had for hours about research and life. I thank all my friends for being there for me whenever I needed them. Finally, I thank my friends at ECU and University Park Apartments for making my stay in Greenville fun and memorable.

Table of Contents

List of Figures

List of Tables

Abbreviations

PrP – Prion Protein

CJD – Creutzfeldt- Jakob's disease

TSEs – Transmissible Spongioform Encephalopathies

GPI – Glycosylphosphatidylinositol

NMR – Nuclear Magnetic Resonance

PrP^{c} – Cellular form of Prion Protein

PrP^{Sc} – Scrapie form of Prion Protein

Cu^{+2} – Copper ion

Zn^{+2} – Zinc ion

K_d – Dissociation constant

EPR – Electron paramagnetic resonance or

ESR -Electron spin resonance

BoPrP – Bovine Prion protein

AFM – Atomic Force Microscopy

CD- Circular Dichroism

MCR-ALS- multivariate curve resolution–altermating least squares

eq. - equivalent

ITC- Isothermal Titration Calorimetry

n- Number of binding sites

K_{eq}- equilibrium constant

ΔG-Gibbs free energy

ΔH- enthalpy

ΔS- entropy

R- gas constant

ACES- N-2-(Acetamido)-2-aminoethane sulfonic acid

SPPS- solid phase peptide synthesis

DMF-*N*,*N*-dimethylformamide

DIEA- diisopropylethylamine

Fmoc- 9-fluorenylmethoxycarbonyl

EDTA-Ethylenediaminetetraacetic acid

HBTU-O-(benzotriazol-1-yl)-1, 1, 3, 3-tetramethyluronium hexafluorophosphate

HOBt-1-hydroxybenzotriazole

TFA-trifluoroacetic acid

TIS-triisopropylsilane

RP-HPLC-Reverse Phase High Performance Liquid Chromatography

ACN- acetonitrile

ESI-Electrospray Ionization

MS-Mass Spectrometry

MCP- micro channel plate

NEM- N-ethylmaleimide

Chapter 1: Introduction

1.1 Overview of Prion Protein and Prion Disease

In the late 20th century, certain infectious particles were found to be responsible for a unique class of diseases. These infectious particles were first identified to cause fatal neurodegenerative diseases characterized by loss of motor control, dementia and paralysis in sheep and goats[1, 2].These particles were named Prions, by Stanley B. Prusiner referring to "proteineous infectious particles". They are caused by deposits of misfolded aggregates of a protein which has novel properties of transmitting the disease in spite of the absence of nucleic acids[3]. The prion diseases include mad cow disease in bovine species, scrapie in sheep and goat, and chronic wasting disease in deer and elk. All the diseases caused by the prion protein were collectively called transmissible spongioform encephalopathies (TSEs). Statistically, TSE's are rare in humans. Some cases of kuru, Creutzfeldt- Jakob's disease (CJD), new variant CJD were seen in humans. Mainly due to their mode of transmission prions are considered as a threat and might lead to a widespread outbreak. This nature of the Prion Protein (PrP) still holds interest in this field of research. The normal cellular functional PrP is represented as PrP^{c} which undergoes a conformational change to form PrP^{Sc}. This could be spontaneous, sporadic or inherited. Sporadic TSEs are most common where PrP^{Sc} is formed spontaneously. PrP^{Sc}, the scrapie form is the misfolded protein with β sheet formation. Due to its amyloidogenic nature, it forms aggregates destroying neighboring neurons. The unique feature of this form is its mode of replication. A PrP^{Sc} once formed acts as a template and converts all the nearby healthy normal PrP^{c} into misfolded forms (PrP^{Sc}) though it is devoid of nucleic acids. This ultimately results in

neurodegeneration. Research into the function and mechanism of action of misfolding will provide insight into treatment of these diseases.

PrP is an endogenous protein commonly found in many body tissues. It is present at high levels in the Central Nervous System. The C-terminal region of the PrP is tethered to the outer surface of the cells through a Glycosylphosphatidylinositol (GPI) anchor[3]. The mature form of the human PrP consists of 208 amino acids. NMR studies conducted on PrP revealed that the C-terminal region of PrP (125-230) has globular structure comprised largely of alpha helices and two stranded antiparallel β sheet. The N-terminal of the protein was found to be unstructured (23 -124)[4-7]. So, PrP is categorized as natively unfolded protein[5, 8].

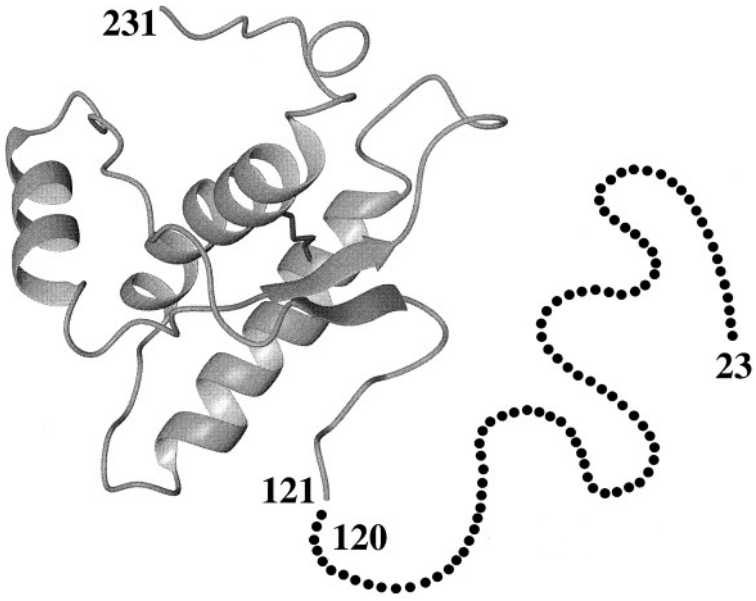

Figure 1.1: Structure of full length PrP obtained by NMR studies[4].

Despite the tremendous research on PrP, its normal function remains unclear. Several experiments were done on PrP knockout mice to determine its function. No remarkable change was observed in the knockout mice making it evident that PrP has a redundant function[9]. It was also observed that the brain extracts of the knockout mice showed lower copper content implying that PrP could probably influence the copper tissue content[10]. The identification of PrP as a copper binding protein led to a majority of the hypotheses on its normal cellular functions. Also, PrP undergoes endocytosis in the presence of Cu^{+2} and Zn^{+2}. Upon exposure to these metals, the PrP anchored to the cell surface is drawn into an endosome into the interior of the cell and then cycled back to the surface of the cell[11-13]. This led to the speculation that PrP might be involved in transporting and storing Cu^{+2} ions thus participating in copper homeostasis. Alternatively, it is also argued that PrP is involved in antioxidant activity due to its capacity to dismutase superoxide and detoxify O_2^- [14].

1.2 Structural Details of the Prion Protein and Copper Binding

As mentioned earlier in the chapter, NMR studies on the recombinant form of PrP revealed that the mature form of human PrP (23-230) consists of a highly globular C-terminus (125-230) with three alpha helices and two antiparallel β sheets. The N-terminus (23-124) lacks any detectable secondary structure. The flexible N- terminus contains four repeats of octapeptide sequence PHGGGWGQ (60-91)[15] followed by GGGTH (92-96) as shown below.

WGQ(**PHGGGWGQ**)$_4$**GGGTH**NQ

The number of octarepeats may vary between species but it is the highly conserved portion of PrP sequence[15]. It was observed that peptide constructs devoid of the octarepeat region do not undergo endocytosis that is stimulated by Cu^{+2} [16]. PrP binding to copper in vivo provides good evidence that it is a copper binding protein. Thus, PrP has been identified as a copper binding protein[17, 18].

The metal binding region of PrP resides in the flexible N-terminal domain as most of the copper dependent responses measured are clearly linked to this region[17, 18]. Hence, the N-terminal region is of great interest. The N-terminal region is highly selective to Cu^{+2} with K_d's ranging from low micromolar to nanomolar range[19, 20]. Thus, PrP has a lot of competition for Cu^{+2} under physiological conditions.

Mass spectrometry and several other studies using different techniques have revealed that at a pH of 7.4 PrP is capable of binding up to five copper ions [19]. Figure 1.3 represents a PrP loaded with five coppers. Cu^{+2} binding to PrP is pH dependent. At a pH of 6, it binds to only two Coppers[19].

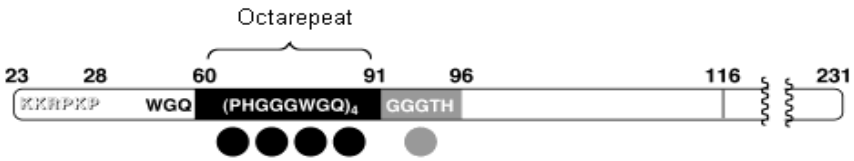

Figure 1.2 Location of the five main copper binding sites of PrP. Spheres represent Cu^{+2} ions[24].

When the octarepeat domain is fully Cu^{+2}–loaded each octarepeat binds a single Cu^{+2} ion[21]. Studies involving electron paramagnetic resonance spectroscopy (ESR or EPR) and X-ray crystallography show that the pentapeptide segment HGGGW constitutes the minimum Cu^{+2} binding unit as shown in Figure 1.4 [22,23].

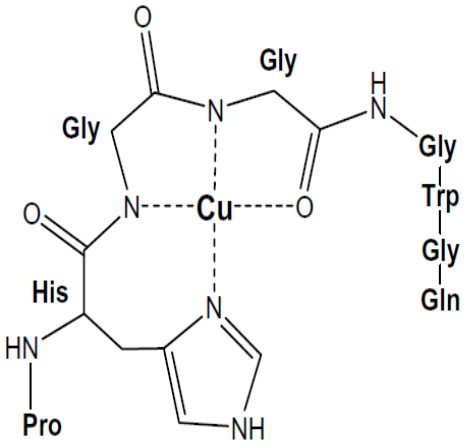

Figure 1.3 Bond line model of the HGGGW-Cu^{+2}complex[24]

The ligands involved in the coordination complex are the nitrogen from the histidine imidazole ring, deprotonated amides from the following two Glycine residues and carbonyl

oxygen from the second Glycine in square planar arrangement. A line-bond structure was proposed based on EPR and X-ray crystallography data[23].

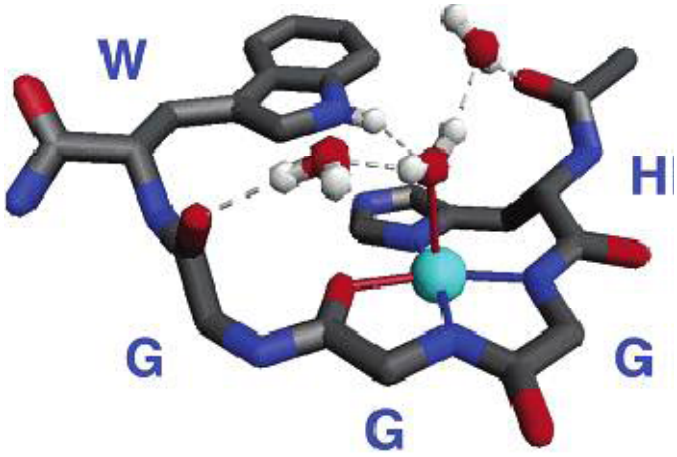

Figure 1.4 Crystal Structure Model of HGGGW- Cu^{+2} complex[23].

The crystal structure represented in the figure 1.4 also reveals axial coordination to a water molecule which participates in hydrogen bond with the indole ring of the tryptophan.

As discussed earlier mass spectrometry data revealed that a fully loaded PrP binds five coppers. If four octarepeats binds to a copper each that accounts for four coppers, further studies were done on full PrP to reveal another copper binding site. Based on studies on recombinant PrP the fifth binding site composed of residues GTH (94-96) was proposed[24, 25].

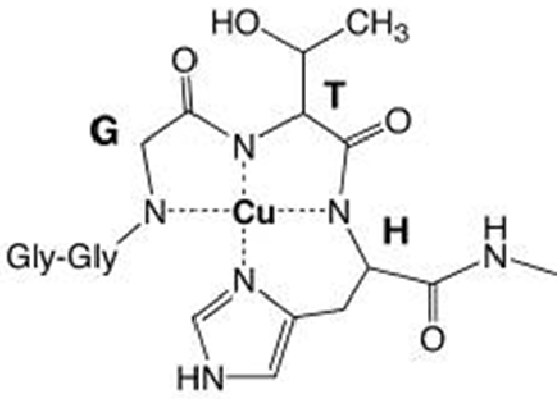

Figure 1.5: Line-bond model for the fifth binding site in PrP[24].

As indicated in the above figure the imidazole ring from the histidine and deprotonated amides from histidine, threonine and glycine contribute the nitrogen ligands[24].

Although PrP is capable of binding up to five coppers, the copper coordination environment at low Cu^{+2} loadings is different from that at high Cu^{+2} loadings. Later research focused on the determining the identity of multiple coordinating complexes possible at sub loaded states. EPR signals were monitored during the titration at various concentrations of Cu^{+2} to determine the various binding modes that exist during titration [26, 27].

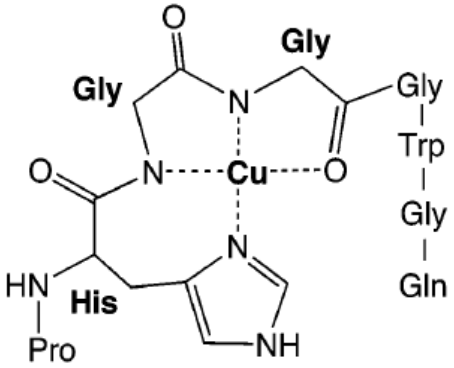

Figure 1.6: Line-bond structure of component 1 of Millhauser's proposed binding model[26].

The first binding mode, component 1 as shown above in Figure 1.6, occurs in a fully loaded state of the protein as discussed earlier.

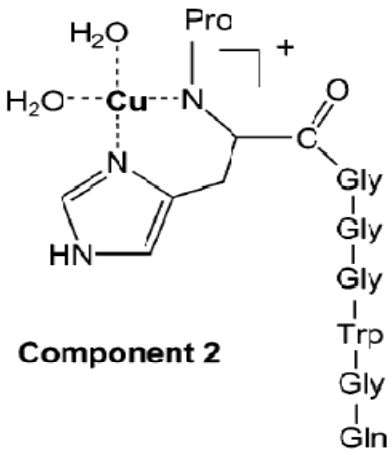

Figure 1.7: Line-bond structure of component 2 of Millhauser's proposed binding model[26].

The binding mode, component 2, requires two adjacent octarepeats and occurs around 1 to 2 equivalents. The ligands involved in this component are N-terminal amide of histidine, amine of the imidazole ring, and two water molecules.

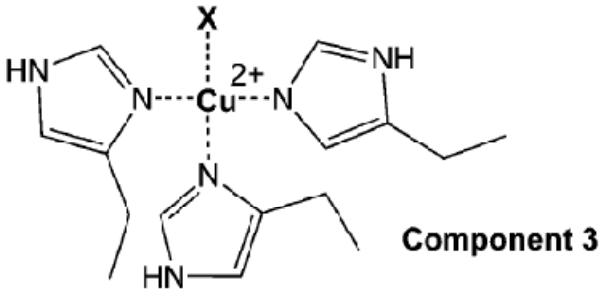

Figure 1.8: Line-bond structure of component 3 of Millhauser's proposed binding model[26].

The other binding component, called component 3, appears at 1 or less equivalents, where the amines of the imidazole ring of histidines and a fourth ligand coordinates a single copper.

All these studies were done on peptide models without the fifth binding site. Figure 1.8 below shows how the proposed modes of Cu^{+2} binding influence the overall structure of the octarepeat region. Component 1 allows the most dynamic structure as each octarepeat binds a single copper. Component 2 allows a semi linear state as two octarepeats bind to a single Cu^{+2} and component 3 shows a more globular structure as three octarepeats bind a single Cu^{+2}.

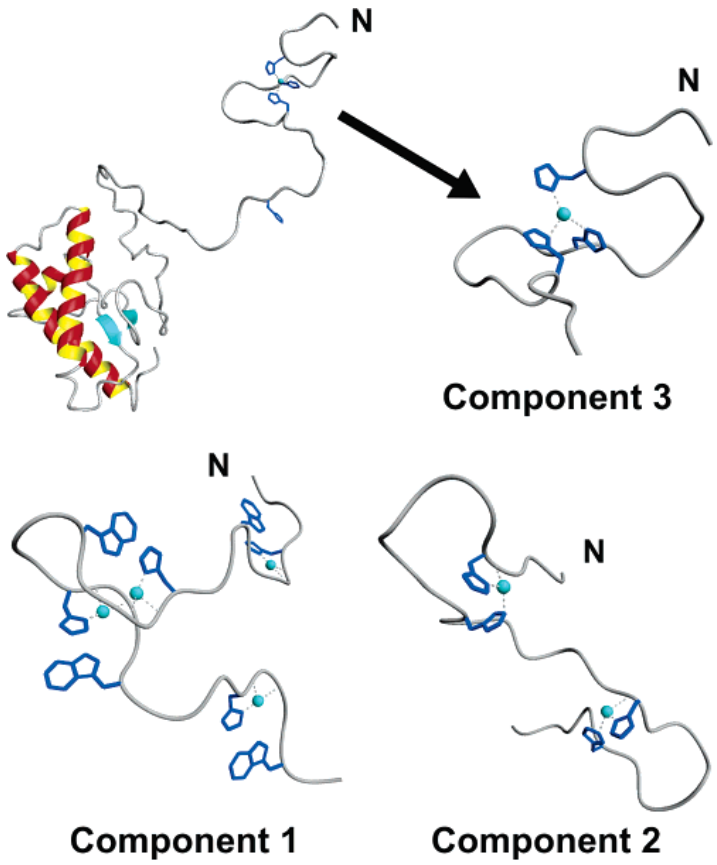

Figure 1.9: Proposed models of different binding modes[26].

1.3 PrP Self-Recognition at Low Cu^{+2} Loadings

One more interesting area is the PrP self recognition at low copper loadings. Work done on full length bovine PrP (BoPrP) indicated that the solutions of protein produced increased turbidity upon addition of copper. Inspection of the insoluble material by atomic force microscopy (AFM) revealed an amorphous mass of PrP- Cu^{+2}complex. Based on these results it was concluded that PrP molecules were oriented in a parallel fashion with Cu^{+2} cross linking them[28]. Further research using Xray absorption spectroscopy on numerous octapeptide models, found that a fully Cu^{+2} loaded BoPrP behaves differently from the half loaded Cu^{+2} [29]. At half site occupancy, that is 3 equivalents of copper (as bovine species have 5 octarepeats), two histidine residues were coordinating a single Cu^{+2} as shown the figure 1.9.

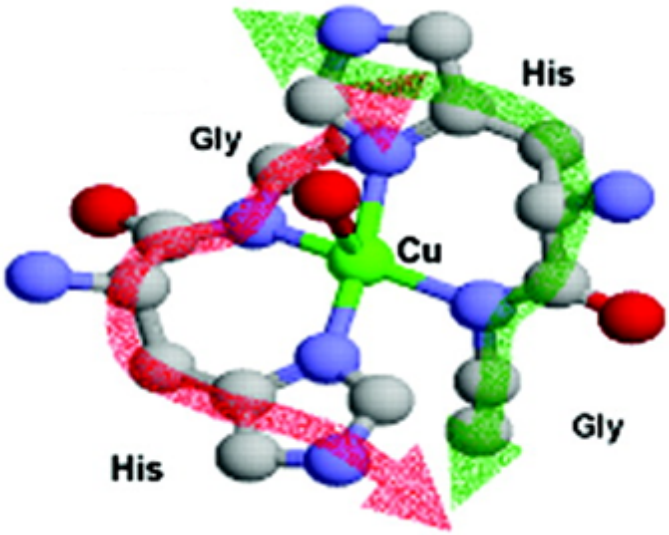

Figure 1.10: Half site occupancy in BoPrP showing the coordination of a single Cu^{+2} by two octarepeats[29].

Increasing the Cu^{+2} /peptide ratio led to rearrangement of the copper coordination sphere, where a single histidine bound each copper ion as shown in the figure 2.0.

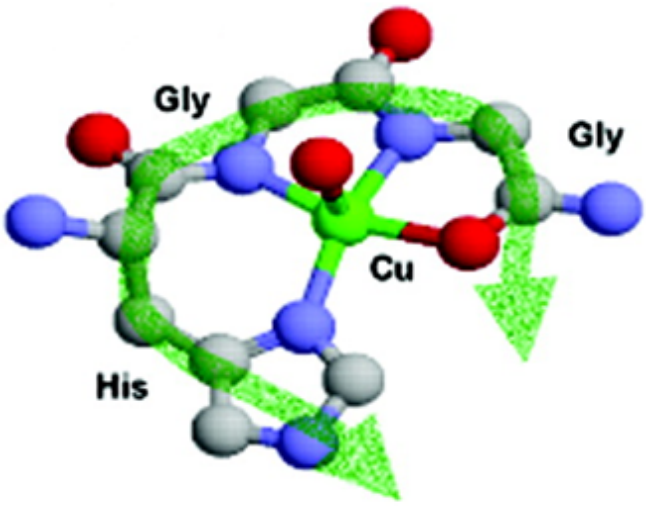

Figure 1.11: Fully loaded Bo PrP representing coordination of a Cu^{+2} by a single octarepeat[29].

Finally, it was proposed that the coordination of a single Cu^{+2} by two histidine residues from different PrP molecules provides a mechanism for PrP cross linking at low copper occupancy (see figure 1.9). These studies were done on peptide models which lacked the fifth binding site but the fifth binding site plays an important role in copper binding. The following macroscopic mechanism was proposed based on these results.

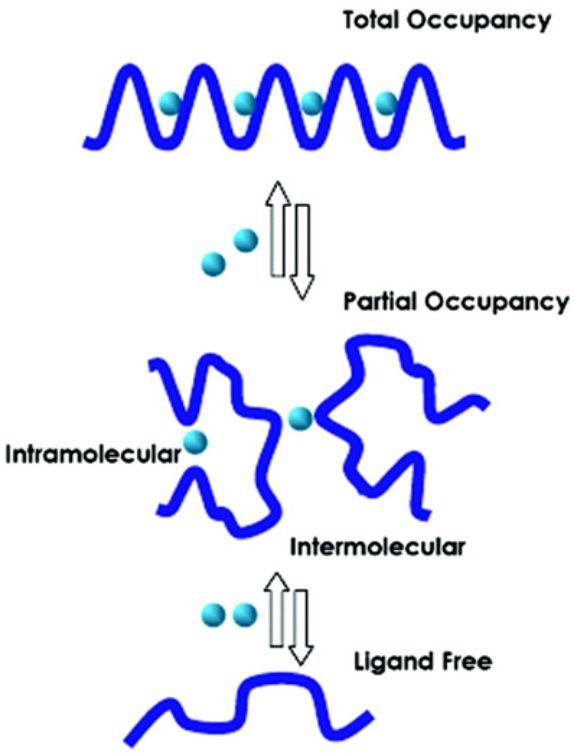

Figure 1.12: Proposed macroscopic process of copper binding in PrP[29].

At very low copper concentration, there are high chances of forming intermolecular bonds which rearrange to form intramolecular bonds when the PrP is fully saturated with copper. This could be a possible mechanism for PrP- PrP interactions through metal cross-linking.

So far a lot of information regarding binding sites and coordination complexes of copper has been obtained and most of the research done didn't involve the fifth binding site. It is believed that the last binding site plays an important role in the cooperativity of the entire molecule. Research done in our lab indicates that the fifth binding site plays a very important role in the early stages of copper uptake. Circular Dichroism (CD) experiments were done on the PrP (57-98). CD Spectra of the titration were analyzed using the self-modeling curve resolution method multivariate curve resolution–alternating least squares (MCR-ALS). The CD data is

discussed in detail in Chapter 4. If the normalized CD intensity is plotted against the equivalents (eq.) of copper added a titration plot is obtained as shown in Figure 1.13.

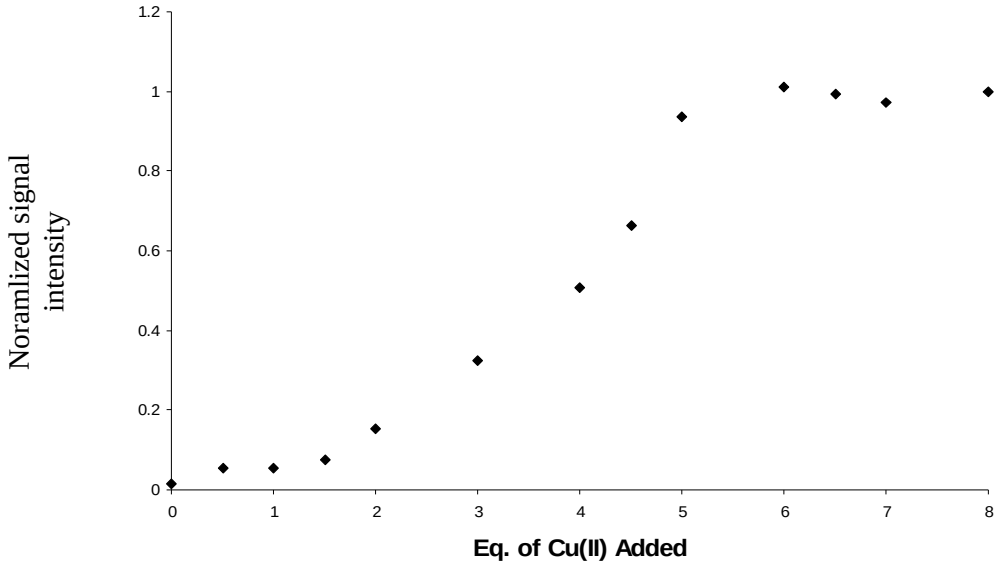

Figure 1.13: Integrated CD signal as a function of Cu^{2+} titrated in PrP peptide in 10 mM NEM at pH 7.4[30]

The titration is sigmoidal with only small gain in the signal until 1.5 eq. representing a CD inactive mode. At low Cu^{2+} occupancy (<1 eq. of Cu^{2+}), coordination is by multiple histidines as shown in Figure 1.7. At intermediate Cu^{2+} occupancy, there is a competition between the multiple histidines and the 5th binding site for Cu^{2+} and the later saturates first and by 5 eq. of Cu^{2+} all the individual octarepeats are loaded. Thus, the 5th binding site is involved early on in the binding process and is saturated before all the individual octarepeats.

Some more research done in our lab also indicates that Cu^{2+} and Zn^{2+} increase the level of PrP- PrP interactions[31]. Studies were done on PrP models incorporated on the outer surface of liposomes through fluorescent lipophilic anchors. On addition of metal, a change in the fluorescence signal was observed due to close proximity of the fluorophore in the lipid bilayer as

shown in the figure 2.3. When close proximity to each other the anchors, pyrene molecules, form excimers which have a distinct florescent signal compared to the monomers.

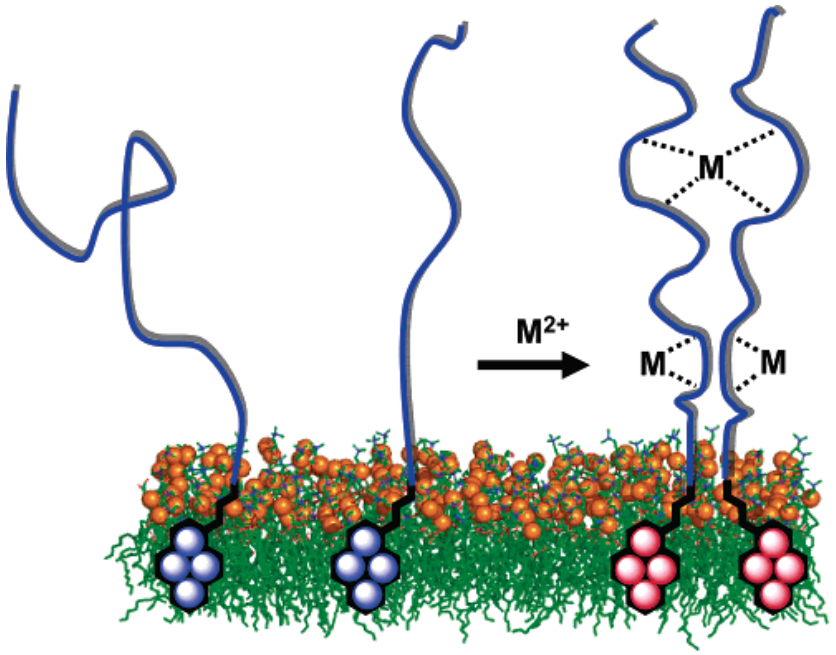

Figure 1.14: Illustration of influence of metal on PrP- PrP interaction[31].

Thus, self recognition of PrP molecules is influenced by the added metals [31].

1.4 Project Design

The ultimate goal in the field of research involving PrP is to understand the PrP – metal binding at a molecular level that might lead to determination of the function of the cellular protein and the mechanism of the formation of the aggregates for the hopeful treatment of the diseases caused by them.

In the present project, we are interested in the thermodynamic aspect of the copper binding to the PrP. The objective of this research is to obtain the thermodynamic profile of the copper- PrP binding; especially at low copper loadings. Further, it may shed light on the advantages of having an unfolded metal binding region.

In the direction of the research goal we used Isothermal Titration Calorimetry (ITC) to obtain the thermodynamic profile of the binding process. ITC can accurately quantify all the thermodynamic properties stoichiometry of the interaction (n), the equilibrium constant (K_{eq}), the free energy (ΔG), enthalpy (ΔH) and entropy of the binding (ΔS).

Once the thermodynamic contributions of the copper to the PrP are determined from the ITC experiments, an understanding of the mechanism and function of the binding at molecular level is better understood. Each of the thermodynamic parameters will be explained starting with Gibbs free energy (ΔG), which gives information about the favorability of the reaction. A negative ΔG value termed as exergonic corresponds to a favorable reaction where no work is required for the reaction to occur. But in the case of positive ΔG work must be performed from the surroundings for the reaction to proceed. It is termed as endergonic and corresponds to a non-favorable chemical reaction. The ΔG depends on the enthalpy, entropy and the equilibrium constant as shown in the equation below.

$$\Delta G=\Delta H-T\Delta S$$

$$\Delta G=-RTlnK$$

Enthalpy (ΔH) is a measure of the total heat involved in a reaction. An exothermic reaction results in a negative value for ΔH. A positive value of ΔH is indicative of an endothermic reaction. Enthalpy will contribute to the spontaneity of the reaction if it is an exothermic reaction. It depends on hydrogen bonding, van der Waals forces, electrostatic interactions and π/π interactions.

Entropy (ΔS) is a measure of energy dispersion at given temperature and is it a function of disorder. Increase in disorder of a system is represented by increase in ΔS. The equilibrium constant indicates the strength of the binding of the metal to the protein. A larger K value corresponds to a more negative ΔG indicating a stronger binding event and a smaller K value indicates a weaker binding event. A binding constant greater than 1 indicates a favorable reaction. Thus, the thermodynamic data reveal the forces (enthalpic or entropic) that drive the complex formation and the mechanism of action. They even provide information on conformational changes of proteins, hydrogen bonding, hydrophobic interactions, and charge-charge interactions.

One important aspect of the research goal is determining the thermodynamic profile of the PrP copper binding at low copper loadings. Experiments were done earlier on PrP binding, but not much information is available on the low copper loading events. ITC being a highly sensitive instrument helps us focus on the earlier events or the low copper loading events. Under physiological conditions very little copper is available and the concentration is approximated at 10 µM and during neuronal depolarization around 100 µM[20]. Hence, PrP needs to compete for copper with other biological species some of which have higher affinities. In the competitive

environment, copper – prion complex might exist in low copper loadings states. To simulate the physiological conditions we chose a highly competing buffer N-2-(Acetamido)-2-aminoethane sulfonic acid (ACES). ACES, at the concentration used in the experiments, keeps the copper prion complex at low occupancy as discussed in chapter 4.

Chapter 2: Synthesis of Peptide Models

2.1 Solid Phase Peptide Synthesis

Solid-phase peptide synthesis (SPPS) with 9-fluorenylmethoxycarbonyl (Fmoc) protected amino acids was used to synthesize all the peptide models. A linear synthesis strategy was used where each amino acid was added one by one until the target peptide is made. It is the most straight forward way to perform SPPS. Peptides are synthesized on an insoluble polymeric resin. The resin acts as the solid support on which the entire peptide is built. To start the peptide synthesis, the resin is deprotected by a secondary amine as shown in the first step of the Figure 2.1. The deprotecting agent used was 20% piperdine in *N, N*-dimethylformamide (DMF). Removal of the protecting group creates a free amine on the resin which is the reactive group and serves as an anchoring site for the addition of the first amino acid. The free carboxyl group of the first amino acid reacts with the free amine of the resin to form an amide bond (second step in Figure 2.1). The resin has the first amino acid attached while the amine of the amino acid is Fmoc protected. It is then deprotected so it can form an amide bond with the free carboxyl group of the second amino acid. All the coupling steps are aided by the use of a reagent diisopropylethylamine (DIEA). The removal of the Fmoc group and addition of another amino acid is repeated until the target peptide is obtained. Thus, in SPPS the peptide chain is synthesized from C-terminus to N-terminus.

Coupling reagents were used to activate the carboxylic group for attachment to the free amine of the growing peptide chain and allow amide bond formation at room temperature. O-(benzotriazol-1-yl)-1, 1, 3, 3-tetramethyluronium hexafluorophosphate (HBTU) was used as the coupling agent and another reagent 1-hydroxybenzotriazole (HOBt) was used as a catalyst

and to prevent any unwanted side reactions. After the last amino acid is attached its free amine is acetylated. Once the target peptide is synthesized, it is cleaved from the resin using trifluoroacetic acid (TFA), water and triisopropylsilane (TIS). The peptide obtained after cleaving has an acetylated N-terminus and amidated C-terminus.

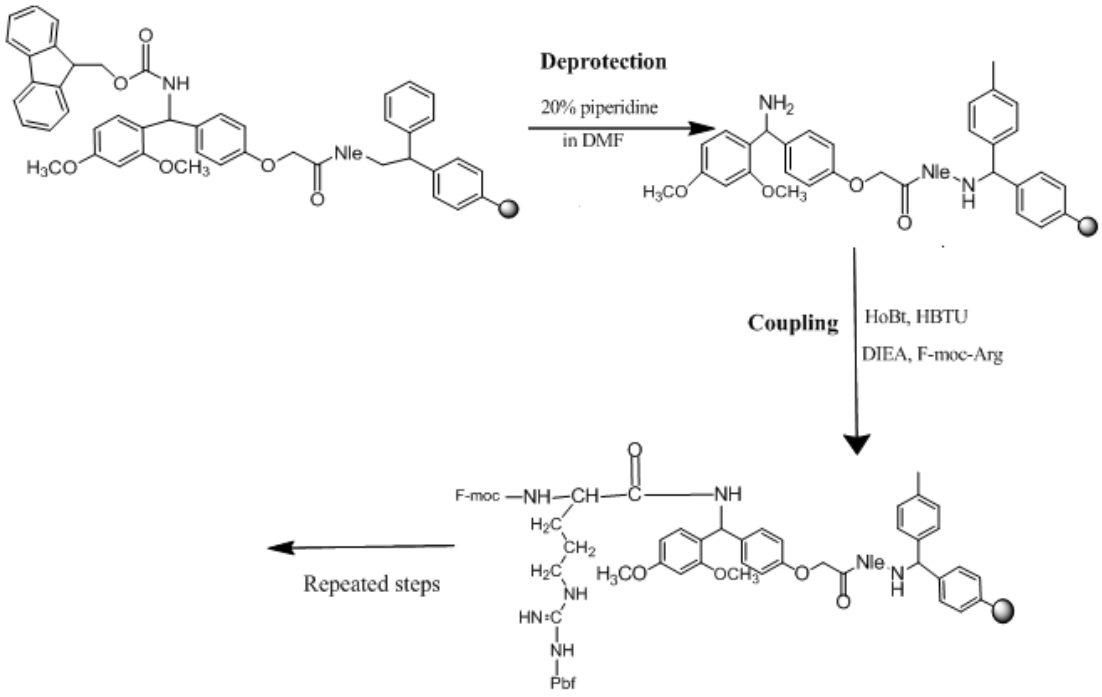

Figure 2.1: Deprotection of the Rink Amide MBHA resin and coupling of amino acids.

2.2 Synthesis of Peptide Models

In the direction of the research goal the first step was to construct the peptide models and then, using these models determine the thermodynamic profiles of their binding interaction with copper by ITC titrations and complement this data by subsequent CD titrations.

Several peptide fragments were synthesized using the principles discussed in chapter 2.1.The small pentapeptide fragment, HGGGW, was used in the initial ITC and CD studies to optimize the experimental parameters though the main peptide of interest was the copper binding region restricted to residues 57-98.

WGQ(**PHGGGWGQ**)$_4$**GGGTH**NQ

In the synthesis of this peptide for the copper binding studies a six amino acid stretch, KKRPKP (23-28), derived from the N-terminus of PrP was added for increased solubility of the overall peptide. It was previously shown to have no effect on the binding of Cu^{+2}. The peptides were acetylated at N-terminus and amidated at C-terminus so that these areas will not coordinate with copper.

Ac-KKRPKPWGQ(**PHGGGWGQ**)$_4$**GGGTH**NQ-NH_2

This peptide model of PrP (23-28, 57-98) consists of 48 amino acids and is expected to serve as a good model for the copper binding region of PrP.

Another peptide that was synthesized was the fragment involving the fifth binding site of the PrP. It is a 10 mer peptide and had the GGGTH site which has been shown to be involved in copper binding.

Ac-WGQGGGTHNQ-NH_2

All the peptides synthesized had tryptophan(s) whose side chain absorbs at 280 nm with a known extinction coefficient. This aids in determination of the accurate concentration of the synthesized peptides spectrophotometrically.

The peptides mentioned above were prepared on a 0.1 mmol scale. The automated synthesis started with swelling 0.1 mmoles of Rink Amide MBHA Resin with the solvent DMF for 30 minutes. The resin was then deprotected with 20% piperdine in DMF twice for 5 minutes. The first amino acid was then coupled using DIEA, HBTU and HOBt. Each coupling step was given an hour. After several washings with DMF, the N-terminus of the first amino acid was deprotected and thus the coupling and deprotecting steps were repeated till the desired amino acids were attached to the growing peptide chain. Once the last amino acid was coupled and deprotected, it was acetylated with approximately 2 mL of acetic anhydride for about 30 minutes. All the amino acids and reagents used were 4 equivalents excess with regard to the amount of the resin used. The Fmoc protected amino acids with the side-chain protecting groups, if applicable, used for the synthesis are listed in the table in next page.

Table 2.1: List of Fmoc protected amino acids with the side-chain protecting groups.

	Protected amino acid used		Protected amino acid used
K	Fmoc-Lysine (Boc)-OH	Q	Fmoc-Glutamine(Boc)-OH
R	Fmoc-Arginine (Pbf)-OH	H	Fmoc-Histidine (trt)-OH
P	Fmoc-Proline-OH	N	Fmoc-Aspartic acid (trt)-OH
W	Fmoc-Tryptophan (Boc)-OH	T	Fmoc-Threonine (tBu)-OH
G	Fmoc-Glycine-OH		

At the end of the automated synthesis, the peptide obtained is still attached to the resin. The peptide is rinsed with methanol and dichloromethane several times alternatively to get rid of any DMF from the synthesis process. It is treated with approximately 8 mL of TFA and 250 µL each of water and TIS which act as scavengers to prevent side reactions. This treatment cleaves the peptide from the resin and removes all the side chain protecting groups. The entire solution is kept aside with intermittent shaking for about 2 hours. The cleaved peptide is treated with ethyl ether. The insoluble peptide precipitates out and is separated by centrifugation.

2.3 Peptide Purification

The peptide obtained after the cleaving was purified using Reverse Phase High Performance Liquid Chromatography (RP-HPLC). A standard non-polar C_{18} column was used and the mobile phases used were acetonitrile and 18 MΩ cm water, both containing 0.1% v/v trifluoroacetic acid (TFA). TFA or any acid added helps to improve the chromatographic peak shape and also provides a source of protons in LC/MS used to characterize the peptide. At a flow rate of 10 mL /minute gradient elution is used to separate the peptides in the crude mixture. A gradient of 100% water and 0% ACN to 0% water and 100% ACN was set for a period of 40 minutes. As seen in the HPLC run below, the peptide peak has atleast two different species eluting as shown by the shoulder on the initial part of the peak. During the collection process the peptide is collected in two different fractions, one before and other after the shoulder in this case. Usually, the fractions collected at a later retention time are purer and are used for experiments. At the end of the HPLC runs peptides of high purity are obtained.

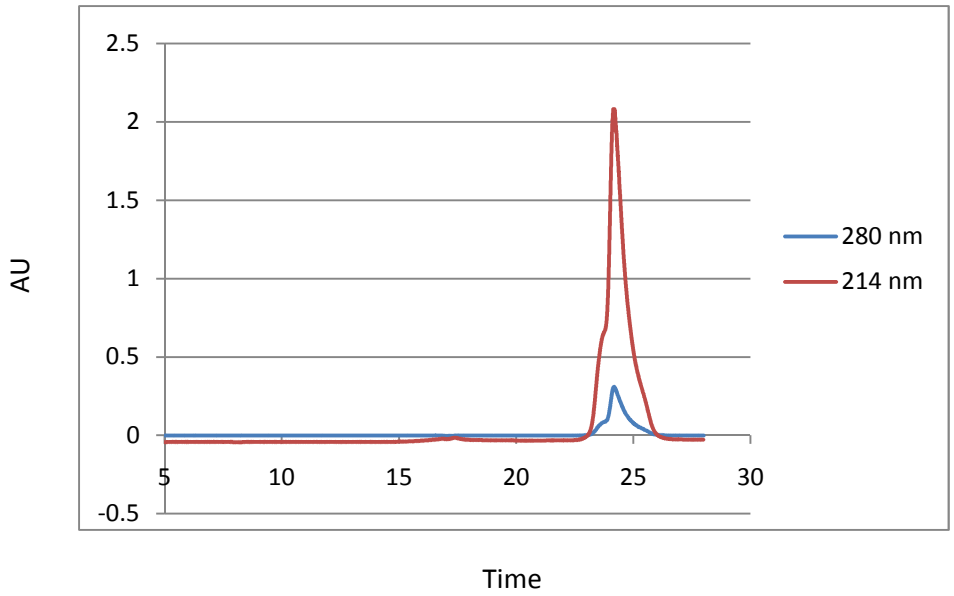

Figure 2.2: RP-HPLC chromatogram on a preparative column of PrP (23-28, 57-98)

2.4 Peptide Characterization

The purified peptides thus obtained were characterized using Electrospray Ionization (ESI) Quadrapole Time of Flight Mass Spectrometry (MS). ESI-MS allows one to determine if the product obtained from a given synthesis has the correct molecular weight. Moreover, this method of MS typically does not fragment molecules during the ionization process, so it called a 'soft' ionization technique. Hence, this is a good technique for analysis of peptides and proteins. The samples were injected to the ESI with a KD Scientific syringe pump at 250 µL/hr and a MCP detector voltage of 2700 V. All conditions were optimized to obtain good signal to noise ratio and least amount of fragmentation. The peptides were analyzed in positive ion mode to interpret the various charged peaks as shown in figure 2.3. Calculation of the deconvoluted mass from the m/z peaks using the formula given below, gives us the observed mass which is comparable to the target mass.

$$m/z = (M+nH)/n$$

Thus, ESI-MS is an excellent characterization technique for the peptides in positive mode. The table indicates the target masses of the peptides synthesized for this project. Sample ESI-MS spectrum is shown in Figure 2.3.

Table 2.2: Target and observed masses of the peptides synthesized.

Model peptides	Target mass	Observed mass
PrP (23-28, 57-98)	4921.3020 Da	4920.8625 Da
PrP (89-98)	1081.4689 Da	1081.7261Da

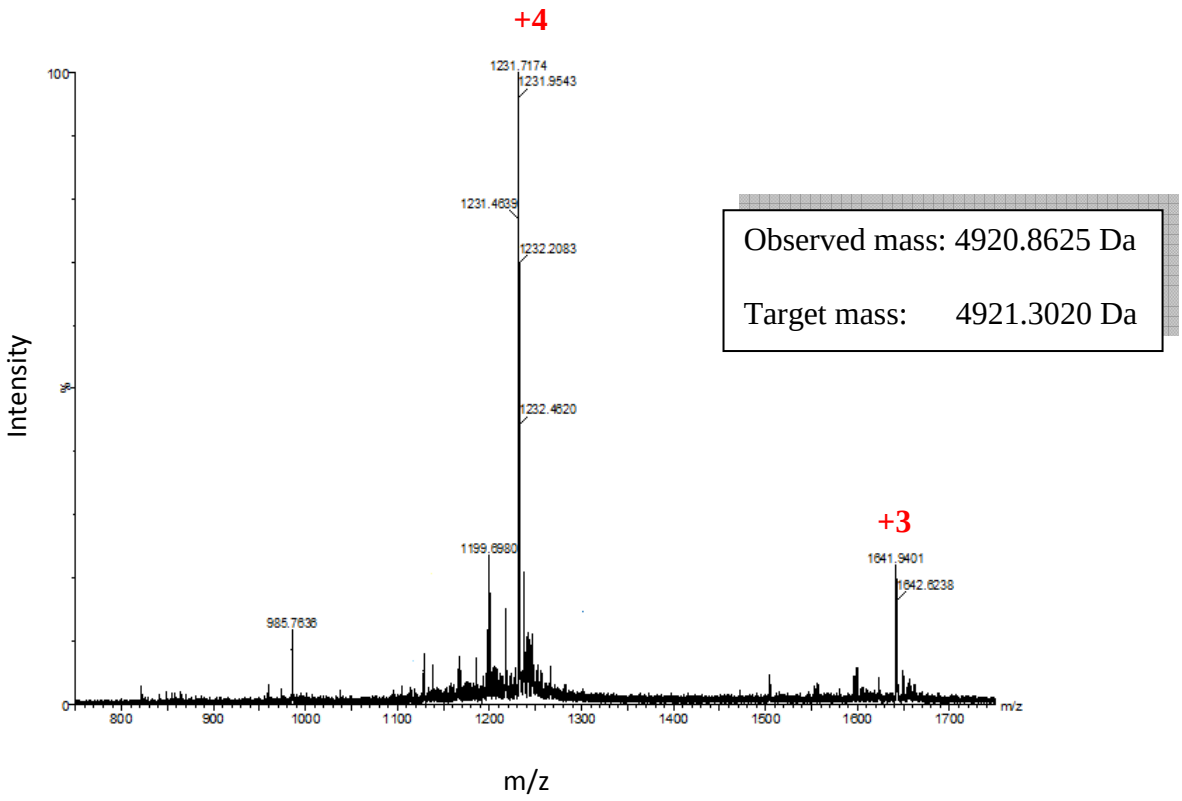

Figure 2.3: An ESI-MS spectrum of PrP (23-28, 57-98) from RP-HPLC.

In the above MS, two peaks of +3 and +4 charge state were observed. The average mass of the two peaks is 4920.8625 Daltons which is very close to the target mass calculated for the PrP peptide (4921.3020). Hence, we know that the peptide synthesized was PrP (23-28, 57-98).

Chapter 3: Thermodynamics Studies: Prion Protein Binding at Low Copper Loadings

3.1: Isothermal Titration Calorimetry

Biological macromolecular interactions, either protein-protein or protein-ligand, are very complex. Understanding the nature of forces that drive or stabilize these interactions is of great interest as a combination of structural information with the energetics of binding can provide a complete picture of the binding process. A measure of the thermodynamics aids in identifying the energetic contributions. The thermodynamics of association are characterized by the stoichiometry of the interaction (n), the equilibrium constant (K_{eq}), the free energy (ΔG), enthalpy (ΔH) and entropy of the binding (ΔS). Here, isothermal titration calorimetry (ITC) is used to obtain the thermodynamics for protein-ligand interactions. ITC is a technique that directly measures the heat evolved or absorbed during a biomolecular binding event. ITC is the most powerful tool that simultaneously determines all the thermodynamic parameters (n, K_{eq}, ΔH) in a single experiment. The free energy and the entropy of the binding can be calculated once the equilibrium constant and enthalpy are known.

General description of an ITC instrument:

An ITC instrument consists of two identical cells made of thermally conducting material. The sample cell is filled with the macromolecule and the reference cell with buffer or water minus the macromolecule. The ligand is in a syringe and is titrated into the sample cell in precise aliquots.

The two cells are surrounded by an adiabatic jacket which is usually cooled by a circulating water bath as shown in the figure 3.1. All through the titration experiment, the components are maintained at identical temperatures. Any temperature difference between the two cells is detected by means of a thermoelectric device, a sensitive thermocouple or thermopile circuit. A second thermoelectric device measures the temperature difference between the cell and the jacket. Heaters located on both the cells and the jacket are activated or deactivated when a temperature difference is detected.

After the entire setup for the experiment is ready, prior to the addition of the ligand, a constant power of less than 1 mV is applied to the reference cell. This signal directs the feedback circuit to activate the heater located on the sample cell. This represents the baseline signal.

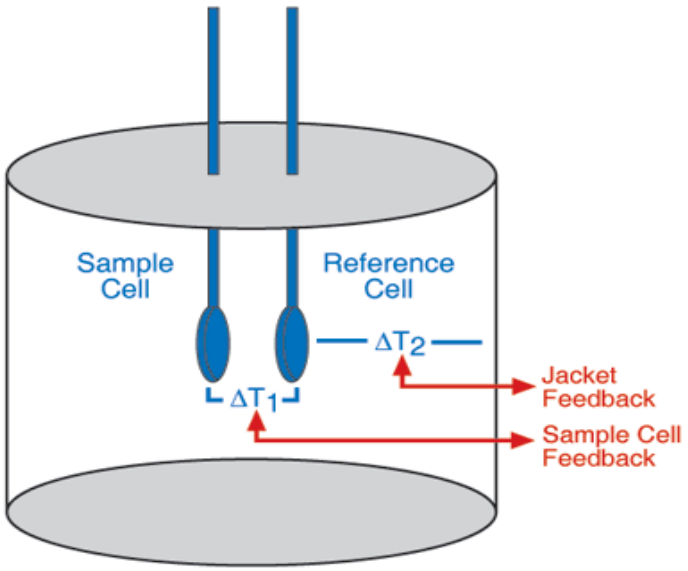

Figure 3.1: Schematic diagram of an ITC instrument.

During the injection of the ligand from the syringe into the sample cell with the macromolecule, heat is evolved or absorbed depending on whether the reaction is exothermic or endothermic. For an exothermic reaction as heat is released, the temperature of the sample cell

increases and so the sample cell feedback is deactivated to bring the two cells to the same temperature. In the case of endothermic reaction, the sample feedback is activated as the temperature of the sample cell is decreased.

The power that is required to maintain the reference and sample cell at identical temperatures is measured as the raw ITC data. This raw ITC data obtained during the titration, a plot of power in µcal/sec as a function of time in seconds, is a series of spikes of heat flow depending on the number of injections of the ligand. An endothermic event gives rise to a positive peak and an exothermic event gives rise to a negative peak. Integration of the heat flow peaks with respect to time gives the total heat in kcal/mole for each injectant which when plotted against the molar ratio (ligand/macromolecule) gives us the binding isotherm, as shown in figure 3.2. Fitting the binding isotherm with an appropriate model gives us the thermodynamic parameters of the interaction under study.

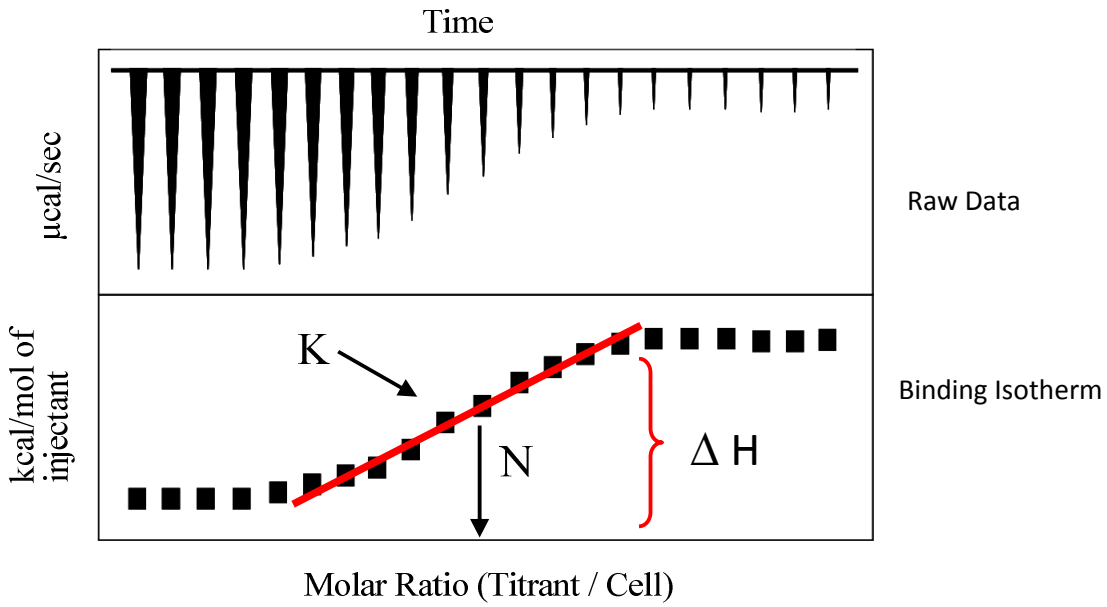

Figure 3.2: Example of an ITC final figure for an exothermic binding event

3. 2: Choice of Buffer for the ITC Experiments

One of the important steps in ITC experiments is the choice of the buffer used for preparation of the samples. Both the macromolecule and the ligand need to be in an identical buffer to minimize the large heats of dilution produced. Large dilution heats could possibly mask the desired observation especially if the binding of the molecules involved is weak. Use of a good buffer is very critical in ITC experiments as the ligand needs to be highly soluble and no precipitation of either ligand or the macromolecule should take place in the sample cell as this may interfere in the heat of the reaction being measured. For the experiments designed in the direction of the research goal, a pH of 7.4 is maintained to be physiologically relevant and also because copper binding to the protein is pH dependent. Most buffers are compatible with ITC and among the buffers available in the pH range, we chose N-2-(Acetamido)-2-aminoethane sulfonic acid (ACES).

ACES is a zwitter-ionic buffer with a molecular formula of $C_4H_{10}N_2O_4S$ and molecular weight 182.2 g/mol (Figure 3.3).

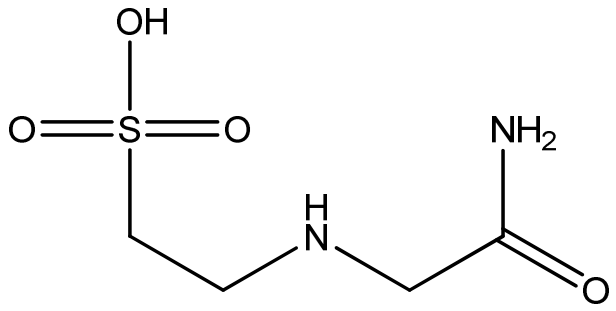

Figure 3.3 Structure of N-2-(Acetamido)-2-aminoethane sulfonic acid (ACES)

ACES was developed in 1960's to provide buffers in the pH range of 6.15 – 8.35 for wide applicability to biochemical studies. The useful range of ACES buffer in aqueous solutions

is 6.1 - 7.5 which is very apt for the experimental setup in this study. ACES is known to form several stable complexes with Cu^{+2}, the metal used in these studies. Formation of any ternary complexes has not been reported[32]. The complex formed depends on the pH of the solution. Although ACES can bind Cu^{+2} in a variety of different ways, this should not interfere with our ITC measurements because we will be measuring the total heat produced by the reaction and we are not interested in describing all equilibria taking place. Some of the complexes of ACES are represented below.

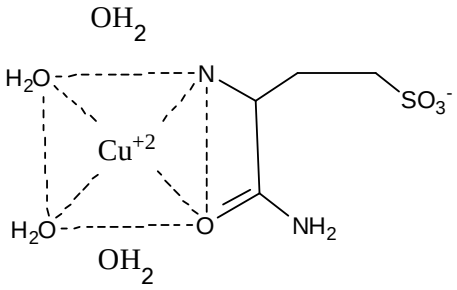

Figure 3.4: 1:1complex of ACES and Cu^{+2} [32].

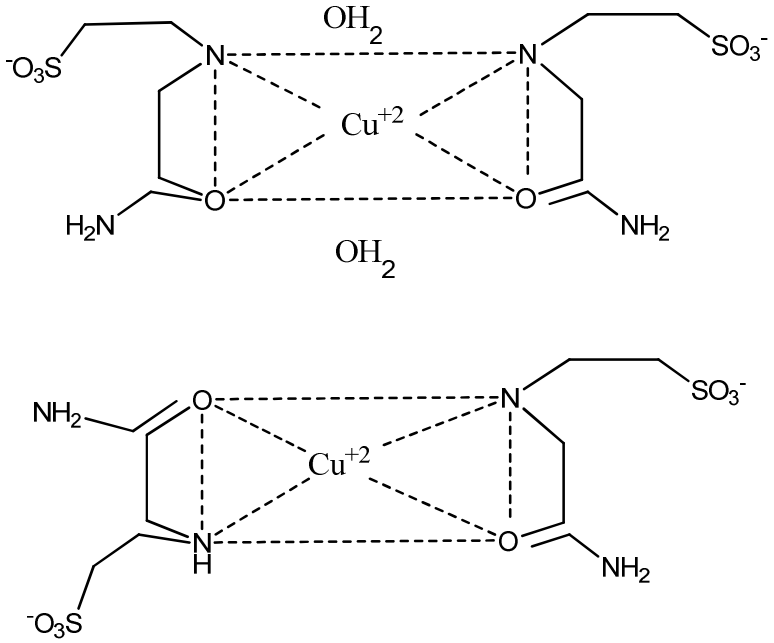

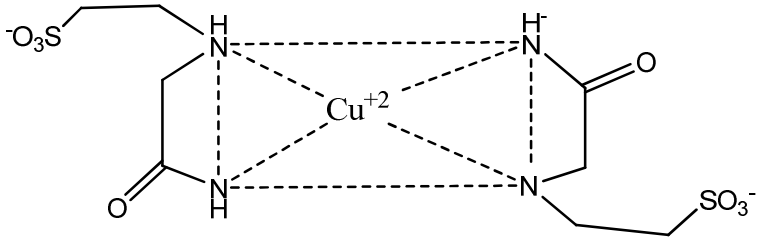

Figure 3.5: 2:1complexes of Cu^{+2} to ACES with different ligating atoms[32]

Since ACES can coordinate Cu^{+2} it should also prevent precipitation of the metal. Two separate 7.5 mM solutions of copper chloride and copper sulfate were prepared in ACES and no precipitation of the metal was found for a period of 48 hours. The optimum concentration of ACES used for the ITC experiments was determined by a set of experiments discussed in the later sections.

3.3 Initial Considerations and Sample Preparation Methodology

All the ITC experiments were performed on a VPP-ITC calorimeter manufactured by microcal. Every step involved in these experiments starting from sample preparation to the data analysis is very crucial and needs to be handled with extreme care given the sensitivity of the technique. A typical ITC experiment involves sample preparation, sample and reference cell loading, injection cell loading, experimental and injection parameters and data analysis.

Sample preparation:

The initial concentration of the macromolecule and the ligand are very critical and need to be determined with high degree of accuracy to get true quantitative data. Ultraviolet-visible absorbance measurements were used for concentration determination of the peptides. All metal solutions were prepared from a concentrated stock solution. All the peptide models tested had trypophan(s) in them and the side chain of this residue has an extinction coefficient of 5690 $M^{-1}cm^{-1}$. Hence, an estimation of the concentration of the peptide stock was possible by using Beer-Lambert's law.

$$A=\varepsilon bc$$

In the above equation A- absorbance, ε- molar absorptivity, b- path length, c- concentration

For the initial experiments, Cu^{+2} was titrated into a solution containing the small pentapeptide fragment (HGGGW), the fundamental binding unit of the PrP in the octarepeat region. These initial experiments helped us to optimize the parameters and also estimate the concentration of ACES buffer to be used.

As HGGGW binding to copper is a simple 1:1 binding event, the experiment was designed to deliver the copper solution in 32 injections where the molar ratio of copper to

HGGGW was 2:1by the end. So, if a 1: 1 binding event occurs, it would produce a titration curve with an inflection point at around 16th injection or data point. With this in mind, solutions of the peptide and copper were prepared. Initially 0.259 mM of copper solution was prepared in 100 mM ACES from a 15.65 mM stock solution of copper sulfate in nitric acid and 0.02 mM of the HGGGW peptide was prepared in 100 mM ACES at a pH of 7.4. Subsequently, the respective concentrations were increased to 0.648 mM copper and 0.05 mM peptide to increase the heat evolved in the titration for better data collection. Both the macromolecule (HGGGW peptide) and the titrant (copper) solutions were prepared in the same buffer to minimize heat from the dilution effect upon titration. The solutions prepared were adjusted to a pH of 7.4 before making up the full volume so no dilution occurs. All the solutions were prepared using 18 MΩ cm water. 18 MΩ cm water is deionized water obtained by using ultrapure mixed resin deionization columns and is devoid of particles greater than 0.2 µm. This confirms that no metals, organics or impurities are contributed from the water.

Loading the Sample cell, Reference Cell and Injection Syringe:

The prepared copper and peptide solutions were filtered using 0.45µm acrodisc filters to remove any precipitated material and were degassed to remove any residual air bubbles. About 1.8 mL's of solution was required to fill the sample cell. Excess was removed with a long needle glass syringe. The working volume of the cell (not including the stem) is 1.460 mL. Any excess solution in the reservoir was removed from the lip of the sample cell. Once the cell is completely filled, several rapid additions of solution help dislodge any residual air bubbles on the sides of the cells. The reference cell is usually filled with 18 MΩ cm water and changed on a weekly basis. Utmost care is required to fill the cells without introducing air bubbles. This is very

important because even the smallest air bubbles in the cell or the syringe can interfere with the feedback current. Moreover, air bubbles give rise to poor baselines[33].

The injection syringe was filled with around 600 µL of the degassed copper solution. Filling the injection syringe with titrant solution also requires great care. Once the syringe is filled, it needs to be loaded into sample cell. Care was taken to avoid bending the needle during this process as some of the titrant may expel into the peptide and thus make the first injection unusable. This is the reason why the volume of the first injection is less (2 µL) than the subsequent injections and this data point is usually discarded. Minor bending of the syringe also leads to poor baselines when the injection apparatus is stirring during the titration. The stirring ensures uniform distribution of the injected titrant into the peptide solution. At the end of the titration typically 258 µL of the copper will have been added to 1.460 mL of the peptide solution.

Experimental Parameters:

The parameters of the titration are input into the software program controlling data acquisition.

Experimental Parameters:

Cell temperature:	25°C
Jacket temperature	25°C
Number of injections	32
Reference power	25µcal/sec

Injection Parameters:

Initial Delay	60 sec
1st aliquot volume	2 µL
Volume of remaining aliquots	8 µL
Stirring speed	307 rpm
Spacing	250 sec

The stirring speed of 307 rpm ensures good mixing and the spacing of 250 seconds between injections ensures that the system reaches equilibrium before the next injection.

Each titration is done in triplicate to check reproducibility. Extensive cleaning is done between the titrations to ensure integrity of the data obtained from the experiment.

ITC Cleaning Procedure:

An extensive cleaning procedure for the peptide models used has been designed after several trial and error methods. The peptides used don't precipitate easily thus avoiding the need for harsh cleaning reagents. Firstly, at the end of the titration, solutions from the cell and syringe are discarded. The sample cell is soaked in methanol for about 15 min and rinsed several times with methanol using a glass syringe to remove any peptide stuck to the walls of the reservoir. To remove any traces of the copper metal in the cell and the syringe manual soaking and rinsing is done with 0.25 M Ethylenediaminetetraacetic acid (EDTA). After this, a cleaning system is set up with vacuum connecting the syringe and the sample cell to a waste bottle. The vacuum flask is attached to the vacuum line through a Thermovac. 50 mL of 2% Contrad detergent solution is run through this system to ensure complete cleaning of the syringe and the cell. Next, 100 mL of

18 MΩ cm water is run to wash away the detergent. The cell alone is cleaned with 400 mL of the detergent and 1 L of 18 MΩ cm water. This cleaning procedure is used at the end of every triplicate run of the same kind of samples.

In between the triplicate runs only manual washing with methanol and, EDTA is done followed by 18 MΩ cm water. Detergent is not used. Sometimes, thorough cleaning of the reaction cell and syringe is done by soaking it with 10% Contrad solution at 65^{o}C for about an hour and cleaned with large amounts of 18 MΩ cm water. A water-water run is performed to make sure that the instrument is ready for use.

Blank Titrations:

The observed binding isotherm is usually plotted as kilocalories per mole of ligand injected and against the molar ratio. The observed heats are apparent heats as they include contributions from dilution of the titrant, dilution of the peptide solution and stirring of the syringe. Blank titrations are performed to correct for heats of dilution[33]. Blank titrations are performed by titrating the titrant or the metal into the 18 MΩ cm water without the peptide in it as 18 MΩ cm is used as a reference in all the experiments performed. For forward ITC titration experiments Cu^{+2} in ACES was titrated into ACES and for reverse titration PrP in ACES was titrated into ACES. These titrations are for precise determination of the heats of dilution which will be subtracted from the binding isotherm before data analysis[33]. The blank was subtracted only in the case of reverse titration for the data analysis shown in chapter 5.

3.4 Initial ITC Experiments

To start, the ITC titration experiments were performed on a small pentapeptide (macromolecule) and Cu^{+2} (ligand). This system has been studied in depth and it is known that a simple 1: 1 complex is formed as shown below in figure 3.6.

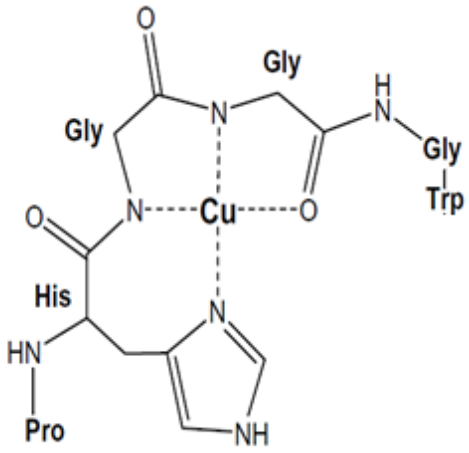

Figure 3.6: Diagram representing the 1:1 complex of HGGGW and Cu^{+2}

Titrating Cu^{+2} into a sample of the HGGGW peptide solution produced the following titration binding isotherms. All the samples were prepared as discussed in section 3.3 in 100 mM ACES and the pH was adjusted to 7.4.

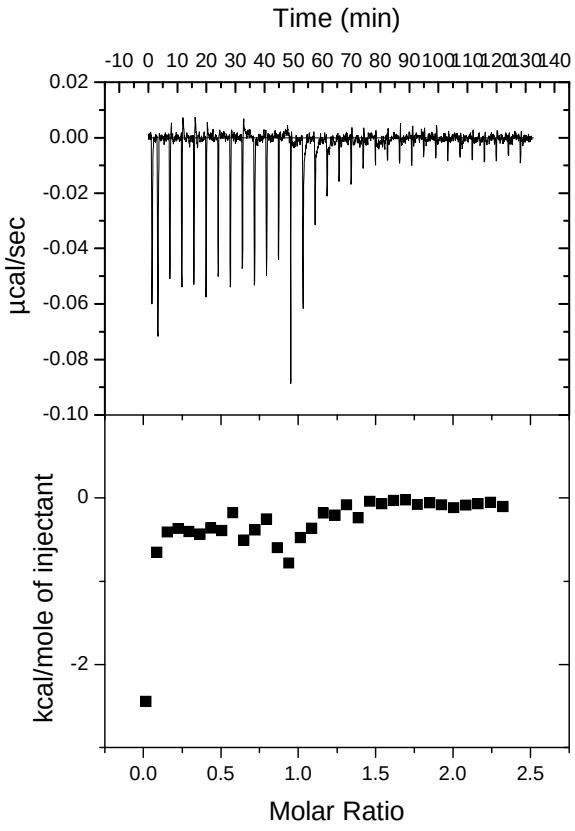

Figure 3.7: ITC titration of 0.259 mM Cu^{+2} into 0.02 mM HGGGW peptide (100 mM ACES pH7.4 at 25^0c).

As seen in the binding isotherm the heat released is close to zero and similar to a buffer run and the triplicate runs that were done for checking the reproducibility were not identical. So, in order to improve the heats involved in the reaction the concentrations of the Cu^{+2} and the peptide were increased and the isotherm in figure 3.8 was obtained.

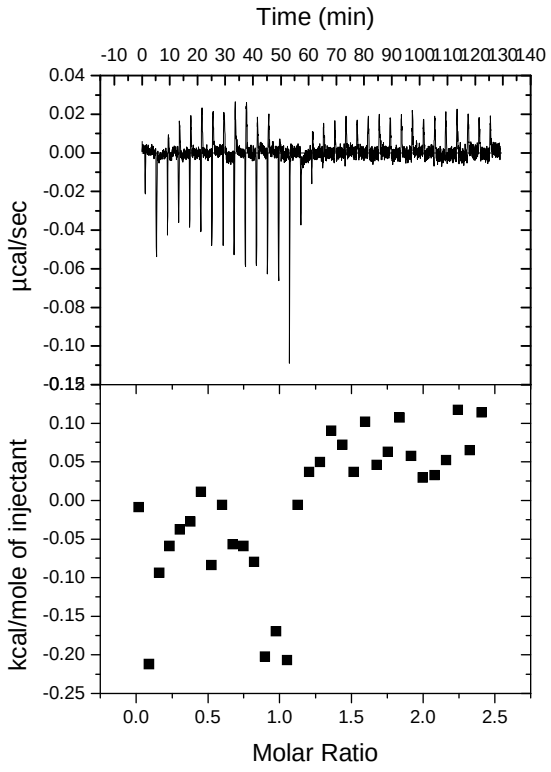

Figure 3.8: ITC titration of 0.648 mM Cu^{+2} into 0.05 mM HGGGW peptide (100 mM ACES pH7.4 at 25^0c).

Improving the concentrations did not give an improved binding isotherm. The graph from these titrations indicated that the expected simple 1:1 complex of the pentapeptide with Cu^{+2} was probably not forming due to the fact that it is a very weak binding event and unable to compete with the complexing buffer. To investigate this, some experiments were done by CD.

3.5 CD Experiments on the Pentapeptide

Due to the unexpected results from the very simple binding process of the pentapetide with Cu^{+2}, this was studied by CD. This system was earlier studied by CD using non-complexing buffers and the signals are well characterized. CD experiments were performed using the sample preparation indicated in section 4.3. All the CD studies discussed in this section were done before optimization of the parameters and so there is significant noise in the spectrum. All the CD data shown are smoothed using Kaleidagraph.

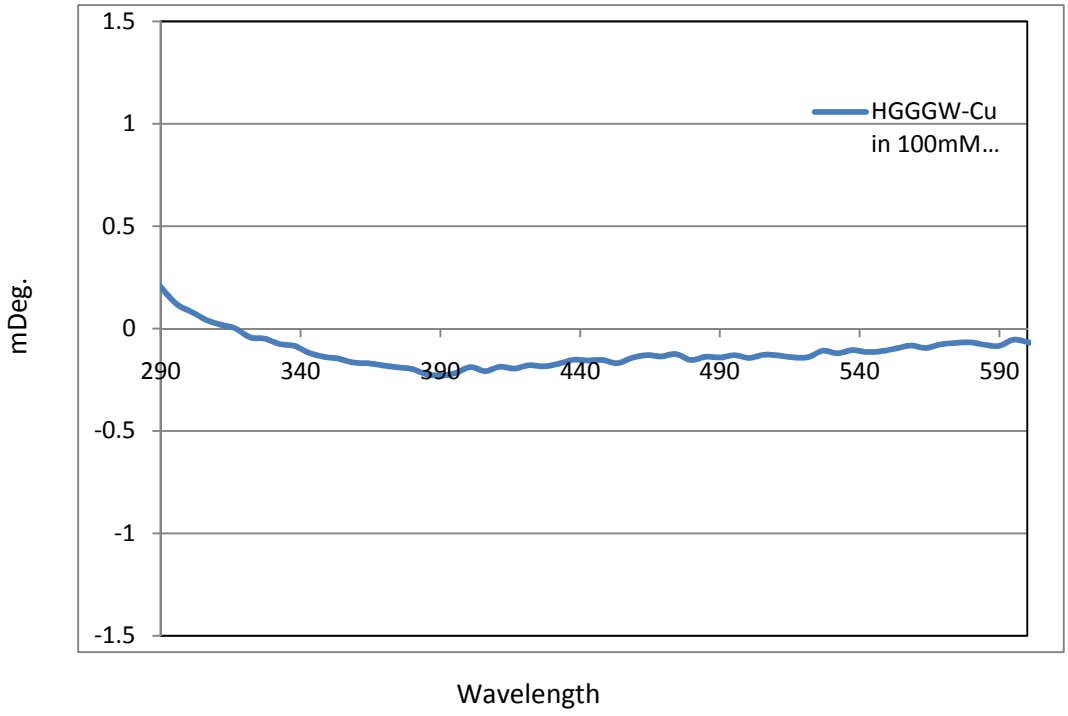

Figure 3.9: CD spectrum of for HGGGW in Cu^{+2} (100 mM ACES, pH 7.4 at 20^0C)

According to the previous CD studies indicated in section 4.2 the pentapeptide should give characteristic positive bands at 330 nm and 588 nm. Figure 3.9 indicates no such band whereas a baseline is observed which indicates that no binding took place. This clearly explains

why the ITC binding isotherms showed no significant changes in heat and thus no apparent binding.

Speculating that this behavior of the peptide is due to high competing nature of the ACES buffer, the CD spectrum for the pentapeptide was obtained in non-competing buffer used in our lab before, N-ethylmaleimide (NEM).The results are shown in figure 3.10.

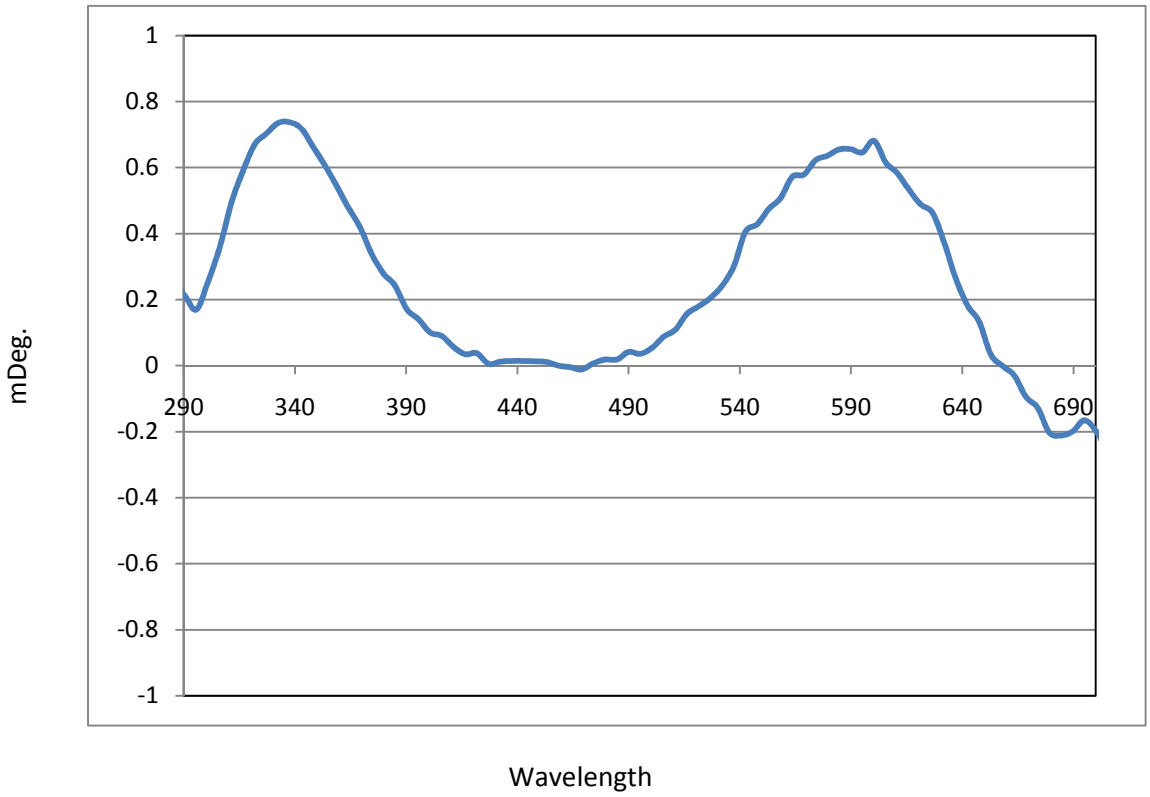

Figure 3.10: CD spectrum for 0.1 mM HGGGW peptide in Cu^{+2} in 10 mM NEM, pH 7.4 at 20^0C

In 10 mM NEM buffer, the pentapeptide showed its characteristic signals at 330 nm and 588 nm indicating the 1:1 complex was formed.To the solution of the complex formed in the experiment in figure 3.10, 100 mM ACES was added. Figure 3.11 shows the spectra of HGGGW- Cu^{+2} before and after addition of 100 mM ACES.

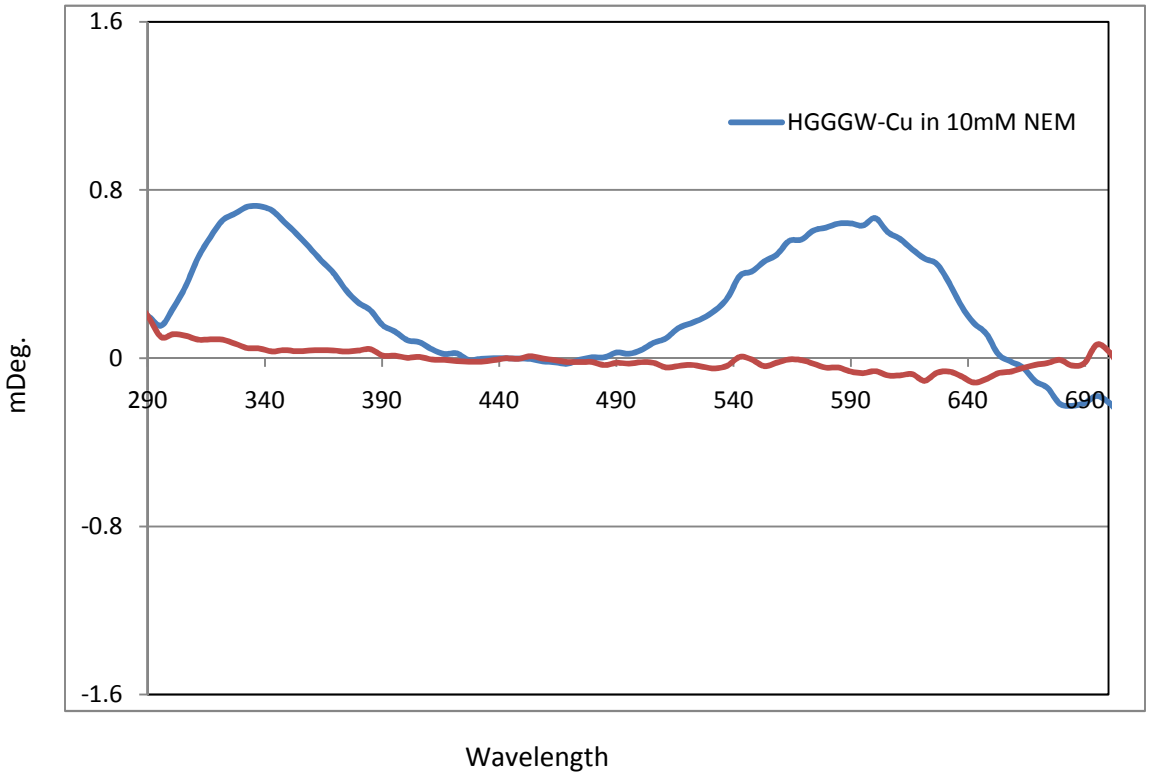

Figure 3.11: CD spectrum of indicating HGGGW- Cu^{+2} before and after addition of 100 mM ACES.

From the spectra it is very clear that, upon addition of the ACES buffer the signal for the 1:1 complex formed between the HGGGW peptide and the Cu^{+2} completely diminishes to baseline meaning that the ACES snatches Cu^{+2} from the complex proving the high competition offered by ACES.

Unfortunately, NEM couldn't be used for the ITC titrations as one of the main criteria was that the copper solutions shouldn't precipitate. So, the concentration of the ACES buffer was reduced to lower concentrations. First 1 mM ACES was used and the characteristic signal at 588 nm wasn't still apparent. Despite this, the optimal concentration of ACES was chosen to be 10

mM as the metal binding region of PrP binds with a higher affinity than the pentapeptide. Due to the high competing nature of ACES in the concentration used we could explore the low copper occupancy. All the subsequent CD and ITC experiments used 10 mM ACES buffer solutions.

3.6 ITC Studies on the N- Terminal Region of PrP (23- 28, 57-98)

After optimization of the buffer concentration (10 mM), experiments were carried out on the N- terminal region of the PrP (23- 28, 57-98) which is represented as PrP in this chapter. The sample preparation methodology for the Cu^{+2} – PrP ITC runs is similar to that discussed in Section 3.3. Changes in the concentration of the peptide and Cu^{+2} or experimental parameters will be mentioned wherever applicable.

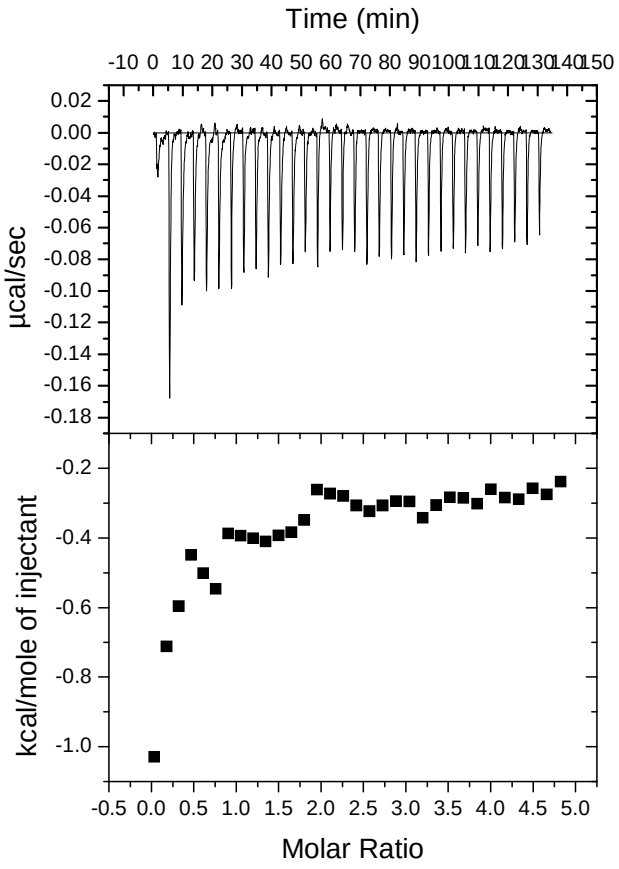

Figure 3.12 ITC titration of 0.909 mM Cu^{+2} into 0.035 mM PrP (10 mM ACES) at pH 7.4 and 25^0C

After synthesizing the PrP using SPPS, a concentration of 0.035 mM solution was prepared in the 10 mM buffer and titrated with a 0.909 mM Cu^{+2} solution. As Cu^{+2}-PrP was done

for the first time on the ITC instrument, an estimate of the heat involved in titration was not available. So, for the first experiment, a reference power of 35 µcal/sec was set. Upon titration of Cu^{+2} (in the syringe) into the PrP (in the cell), the ITC graph shown in Figure 3.13 was obtained.The experiment was conducted at 25°C at a pH above 7. By the end of the 32 injection titration, the molar ratio of Cu^{+2} /PrP was 5.0. From the graph, it is evident that the binding process is purely exothermic. Since the initial data points were not reproducible and the inflection point is not clear, the concentration of protein was increased.

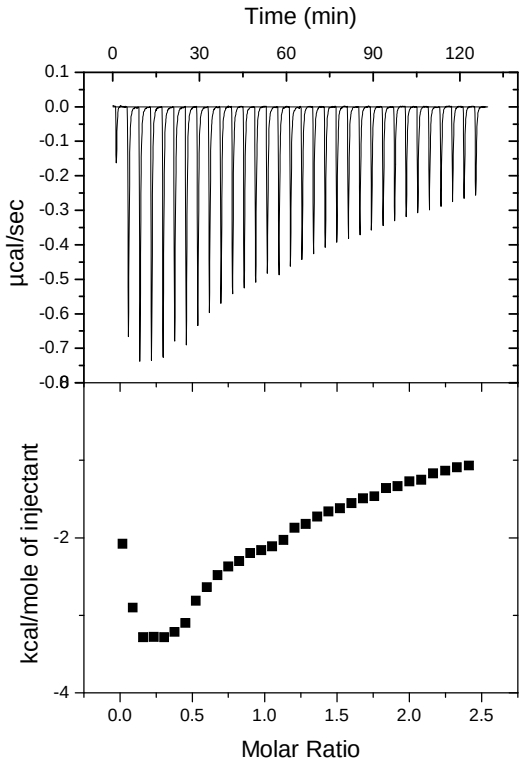

Figure 3.13: ITC titration of 0.909 mM Cu^{+2} into 0.07 mM PrP (10 mM ACES) pH 7.4 and 25^0C.

For the next set of experiments, the PrP concentration was doubled to 0.07 mM to obtain better heats of reaction and to focus on the earlier events. In order reduce the noise, the reference power was reduced to20 µcal/sec. The Figure 3.14 above represents the ITC titration of 0.909

mM Cu^{+2} into 0.07 mM PrP in 10 mM ACES. This titration experiment was so designed so that more data points define the initial part of the titration. By the end of the 32 injection titration the system reaches only 2.5 molar ratio. By increasing the concentration of the PrP better data was obtained. A slight inflection was observed in the initial part of the titration. Since reproducibility was an issue with these experiments the concentration of PrP was increased to 0.1 mM and Cu^{+2} was increased to 1.2 mM.

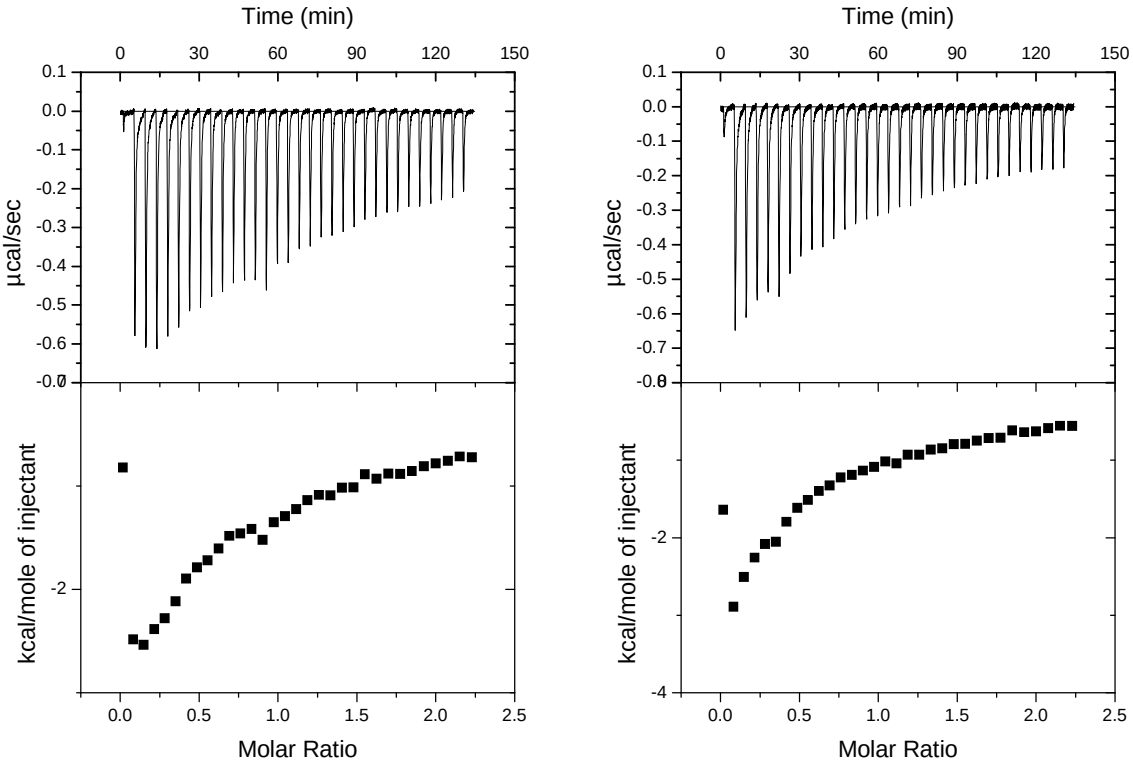

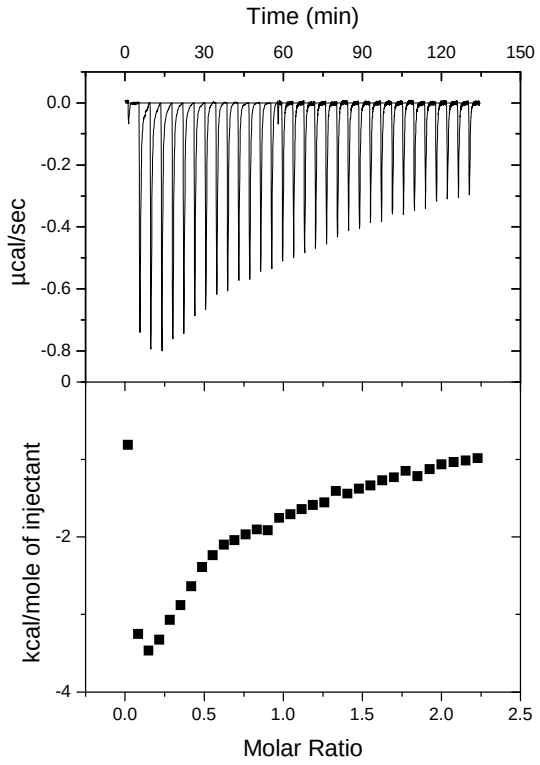

Figure 3.14: ITC titration of 1.2 mM Cu^{+2} into 0.1 mM PrP (10 mM ACES) at pH 7.4 and 25^0C.

In the ITC titration for the data shown above CHELEX-ed water was used instead of nanopure water all through the experiment. It was performed at 25^0C at a pH of 7.5. An interesting observation in this plot was the inflection point at around 0.5 molar ratio. Initially for the first few injections the concentration of PrP is high and very little copper is available for binding. So, based on the binding at 0.5 molar ratio we hypothesized the reaction below occurring initially. Also binding at 0.5 molar may indicate a probability for PrP cross linking at low copper levels.

$$2PrP + 1Cu \longrightarrow PrP_2\text{-}Cu$$

As seen in the above figures reproducibility of the initial part of the titration is difficult to achieve. ΔH is indicative of the total heat involved in the reaction which is the difference in heats between the initial and completion points of the binding event. The ΔH value obtained for these

three graphs is different. In order to obtain a ΔH for these titrations single injection experiments were designed. To measure ΔH by a single injection, requires a c value (defined in the equation below) large enough so the experimental intercept on the isotherm intercepts the Y axis very close to the true ΔH. Since there will be excess macromolecule in the cell, the experimental heat Q will be determined by the amount of ligand injected.

$$c = KM_{tot}n$$

where K is the binding constant, M_{tot} is the total macromolecule concentration and n is the number of binding sites.

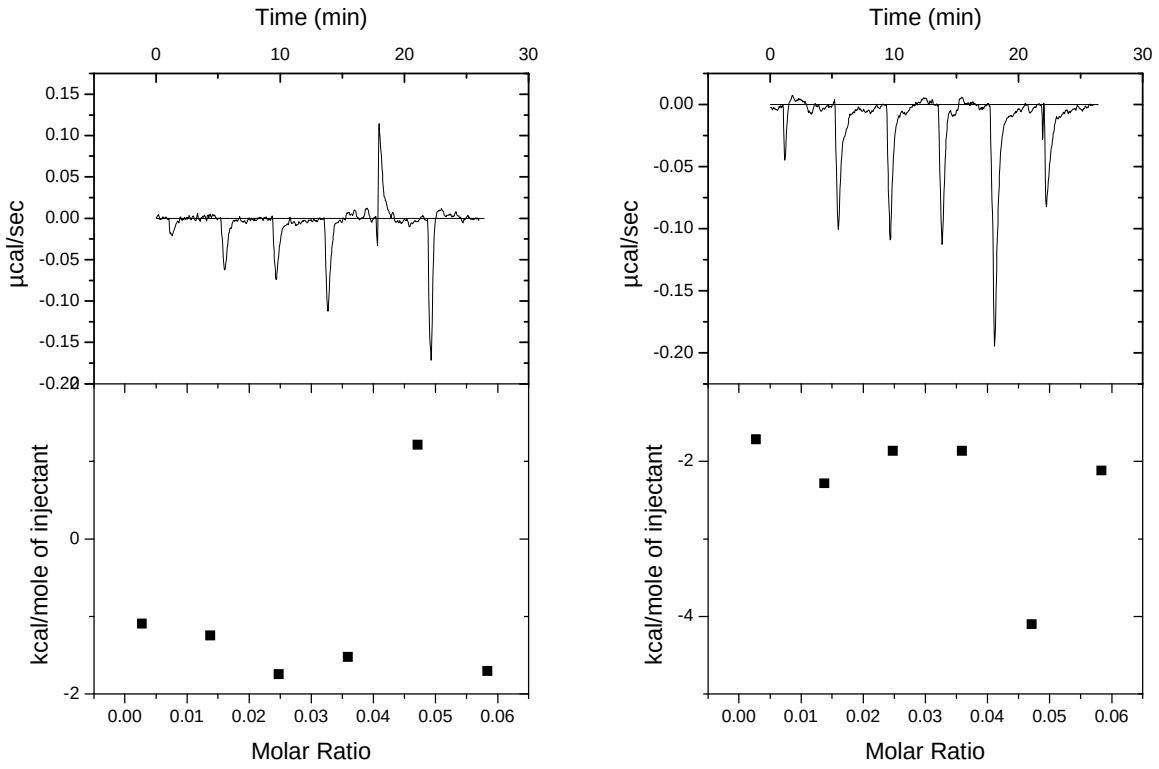

Figure 3.15: Single injection run of 0.2 mM Cu^{+2} into 0.1 mM PrP (10 mM ACES) at pH 7.4 and 25^0C.

0.2 mM Cu^{+2} was titrated into 0.1 mM PrP for the single injection run experiments. It was carried out till 6 injections at 25^0C at pH of 7.4. Two runs of the several runs performed are shown in figure 3.15. Since the data points were scattered we couldn't determine the ΔH from these runs.

Later, concatenated runs were done at the peptide concentration of 0.1 mM and copper concentration of 1.2 mM. It is evident from the previous set of experiments the PrP is not saturated. A concatenated run was planned to reach 5 molar ratio of Cu^{+2} /PrP also retaining the initial part of the titration as it is very crucial. After obtaining the data it was found that PrP wasn't saturated even at 5 molar ratio. This is due to the competition offered by the ACES buffer to the peptide.

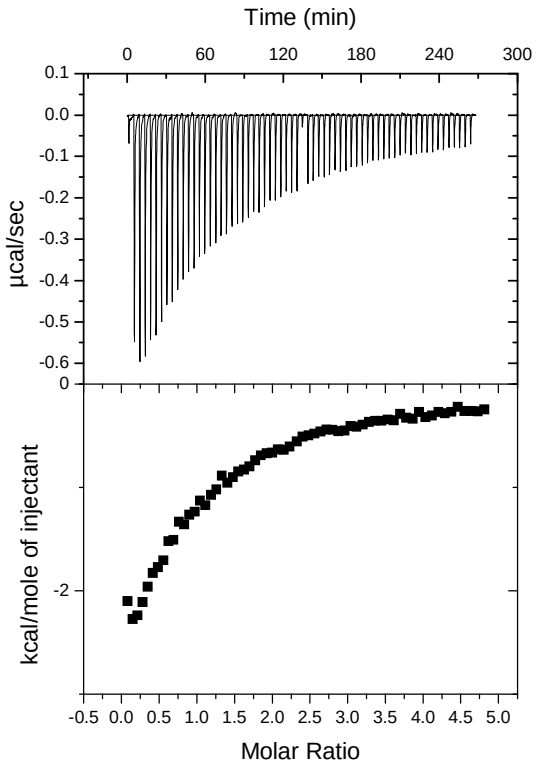

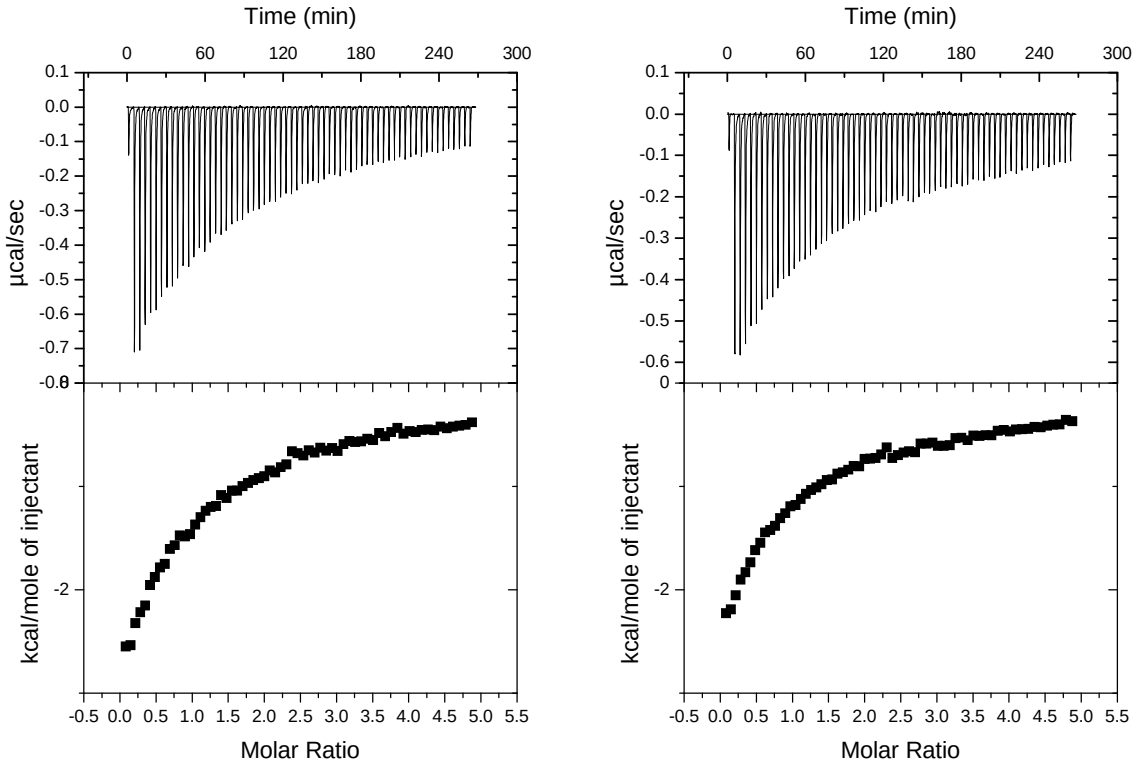

Figure 3.16: Concatenated runs of 1.2 mM Cu^{+2} into 0.1 mM PrP (10mM ACES) at pH 7.4 and 25^0C.

These 64 injection titration runs were done at 25^oC and pH of 7.4. In this case 32 injections were delivered by the first syringe full of Cu^{+2} solution into the cell containing PrP, at the end of which the syringe was filled again with Cu^{+2} to deliver the next 32 injections which makes a total of 64 injections. These titrations were performed in triplicates for reproducibility as shown below.

In the concatenated runs shown above the first injection point of 2 µL is discarded. These concatenated runs were reproducible and were used for ITC data fitting to obtain the thermodynamic parameters.

3.7 Reverse Titration of PrP (23- 28, 57-98) into Cu^{+2}

After successfully obtaining reproducible ITC titration graphs for the forward titration of Cu^{+2} (in syringe) into PrP (in the cell), reverse titrations of PrP (in syringe) into Cu^{+2} (in the cell) runs were executed. These reverse titration data interpreted along with the forward titration data will help find an appropriate model for fitting the data.

Initial reverse titration data was obtained by titrating 0.75 mM PrP into 0.05 mM Cu^{+2} at 25^0C at pH of 7.45. The sample methodology is similar to the procedure discussed in section 3.3.

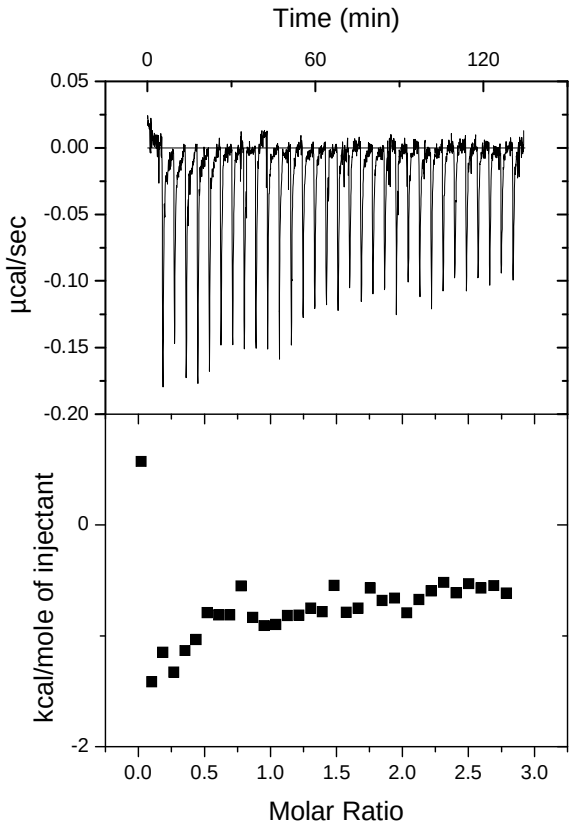

Figure 3.17: Reverse ITC titration of 0.75 PrP in Cu^{+2} (10 mM ACES) at pH 7.4 and 25^0C.

The ITC data obtained from this titration did not evolve sufficient heat. Hence the concentrations were increased and concatenation runs were executed.

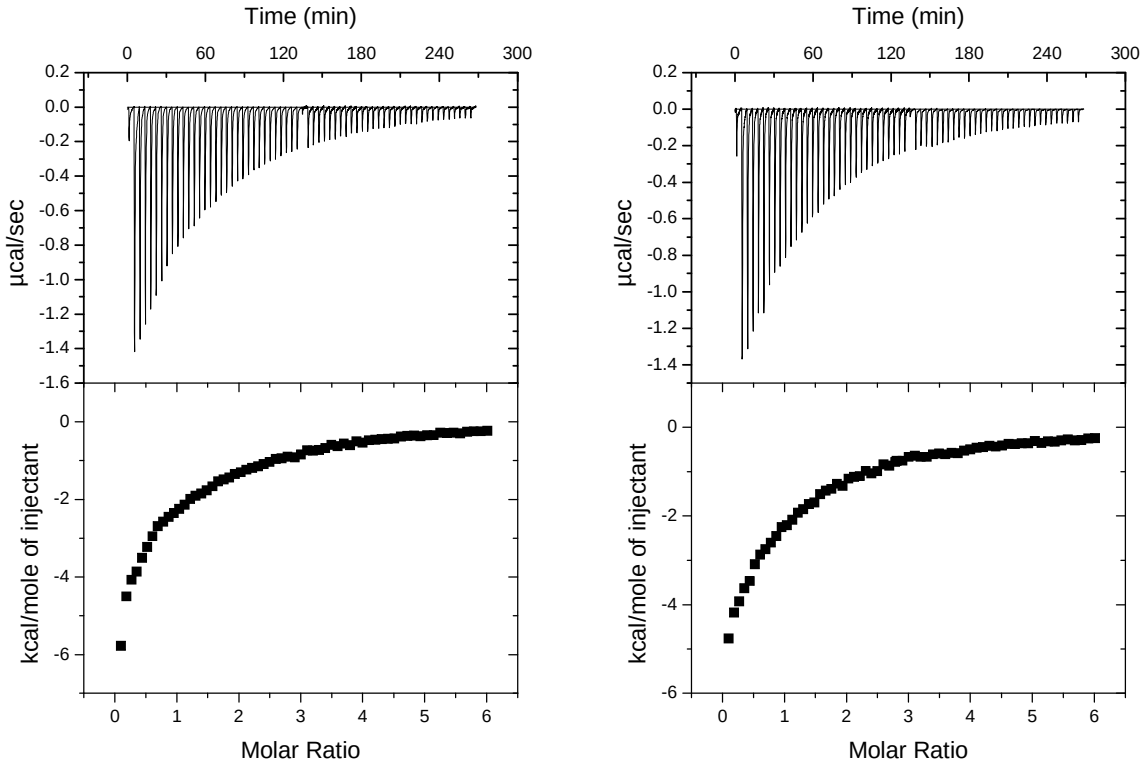

Figure 3.18: Concatenated ITC (reverse) titration of 1.5 mM PrP into 0.1 mM Cu^{+2} (10 mM ACES) at pH 7.4 and 25^0C.

As seen in the figure 3.18, the reverse titration is exothermic and reproducible. The binding isotherm shown above does not include the first injection data point. These two sets of data were used for data fitting for an appropriate model. The molar ratio in reverse titration indicates the moles of PrP/Cu^{+2}. Overlay of the forward titration over the reverse titration showed that the process of PrP- Cu^{+2} binding is a perfectly reversible process as shown in Figure 3.19

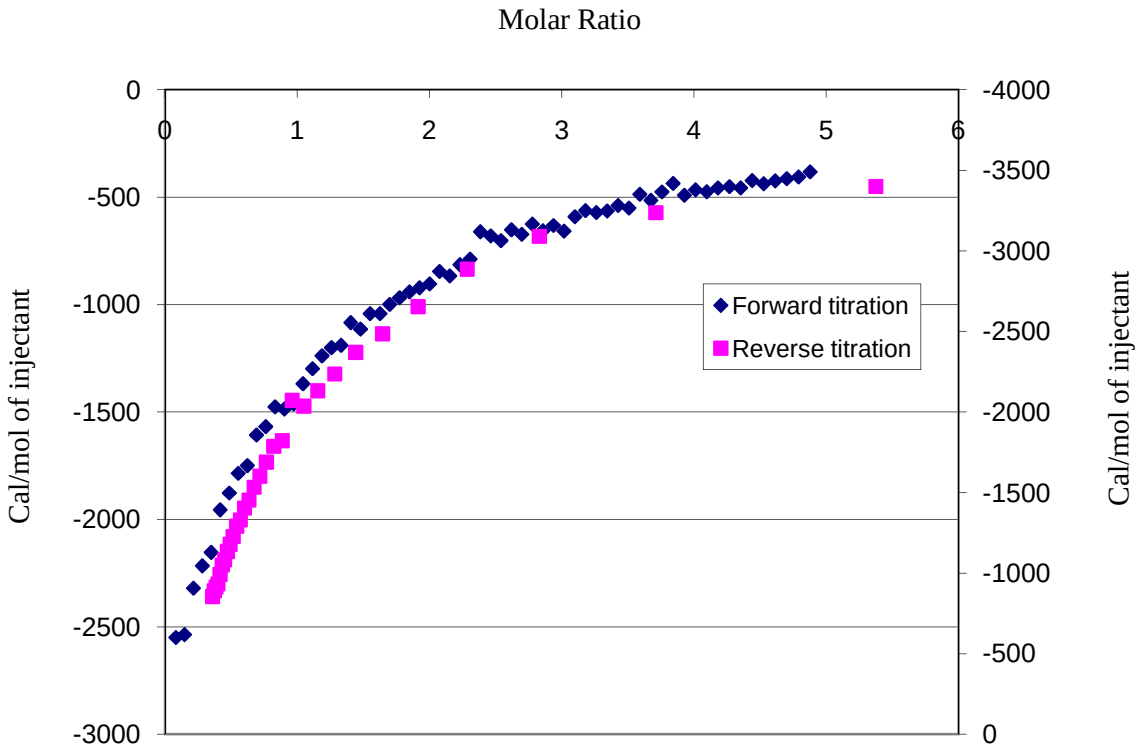

Figure 3.19: Overlay of forward and reverse titration to determine reversibility of the process.

3.8 ITC Titrations on WGQGGGTHNQ (10 mer Peptide)

ITC titrations were done on the fifth binding site (WGQGGGTHNQ). The 10 mer peptide was prepared by SPPS and a solution of concentration of 0.1mM is prepared in 10 mM ACES. 1.5mM Cu^{+2} was titrated into 0.1mM WGQGGGTHNQ in 10 mM ACES as shown in the Figure 3. 20.

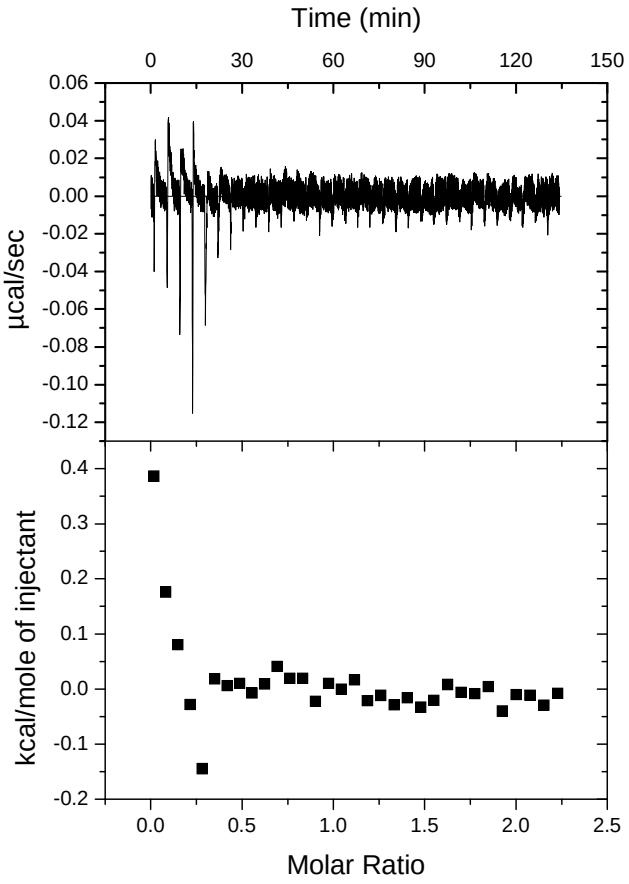

Figure 3.20: ITC titration of 1.5mM Cu^{+2} into 0.1 mM WGQGGGTHNQ (10mM ACES) at pH 7.4 and 25^0C.

Experimental parameters:

Total # of injections	32
Cell temperature	$25^{O}C$
Reference power	15µcal/sec
Stir speed	307
Volume of 1st inj	2 µL
Volume from 2nd inj	8 µL
Injection spacing	250 sec
Initial delay	60 sec

The titration data obtained showed some amount of heat in the beginning of the titration but quickly reached heat of dilution. The amount of heat evolved during the titration was not sufficient enough. The results from this data are inconclusive.

Chapter 4: Circular Dichroism Studies on Copper Binding to PrP(23-28, 57-98)

4.1 Circular Dichroism

The differential absorption of a circularly polarized light by an optically active molecule is referred to as Circular Dichroism (CD).

$$\Delta\varepsilon = \varepsilon_R - \varepsilon_L$$

In the above equation ε_R is absorbance of right circularly polarized light and ε_L is absorbance of right circularly polarized light in the above equation.

In a CD experiment, the chiral sample is subjected to equal amounts of right and left-handed circularly polarized light of a selected wavelength alternately. One of the two polarizations is absorbed more than the other because of the asymmetry of the chiral molecule, and this wavelength-dependent difference of absorption is measured, yielding the CD spectrum of the sample. CD is a very valuable tool with several applications like detection of secondary structure of proteins or conformational changes or measurement of ligand binding. Far UV CD studies help in identification of the secondary structures of proteins whereas; visible CD spectrometry is a powerful tool in investigation of the metal protein interactions. This sensitivity of CD spectra to different ligand interactions in a way is used to measure ligand binding in this project. The metal of interest is Cu^{+2}, a transition metal. Cu^{+2} is a d^9 species that absorbs in visible region due to d-d transitions. These transitions give information about the coordinating ligands and the geometry of the molecule. Any changes in the coordination ligand sphere involving Cu^{+2} can be observed as changes in d-d transitions and thus reflected in the CD spectrum. CD spectroscopy is very sensitive to changes in these transitions even for molecules

with low extinction coefficients. Use of CD spectroscopy for this study has proved to be very useful in terms of estimating the different coordination complexes involved during the titration.

4.2 Previous Circular Dichroism Studies on PrP(23-28, 57-89)

As mentioned in chapter 4.1, CD is used to measure the d-d transitions of Cu^{+2} in the visible region. Any changes in the coordination ligand of Cu^{+2} leads to changes in the absorbed wavelength respectively. Based on these principles of CD, several experiments were performed earlier in our lab where signature absorption bands were assigned to certain coordination complexes of Cu^{+2} with the different binding units of PrP. These signature absorption bands can be used to characterize the extent and mode of copper PrP binding in the present studies.

The PrP peptide (23-28, 57-98) contains 5 binding sites to bind copper as shown below.

KKKRPKPWGQPHGGGWGQPHGGGWGQPHGGGWGQPHGGGWGQGGGTHNQ

Out of the 5 binding sites, typically there are 2 different types of binding sites, the octarepeat region (PHGGGWGQ) which repeats 4 times and the GGGTH residues, the fifth binding site. The fundamental unit of the octarepeat region is HGGGW and that of the fifth binding site is GTH.

Figure 4. 1 below represents the CD spectra of the fundamental units of Cu^{+2} binding in the PrP peptide when fully loaded with Cu^{+2}.

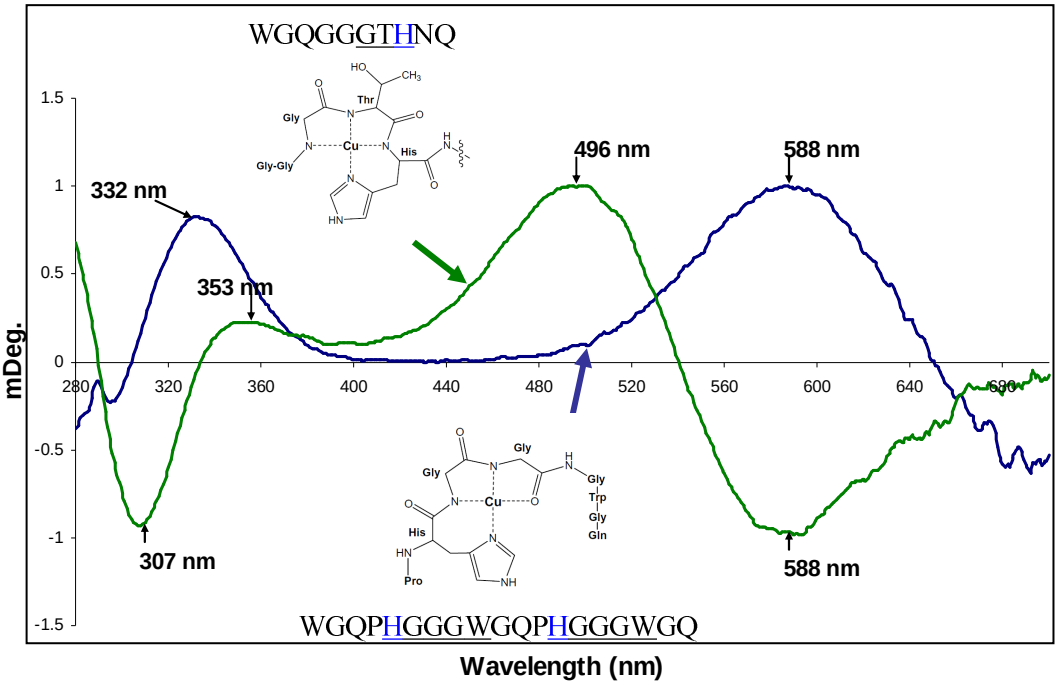

Figure 4.1: CD spectra of GTH binding site and dioctarepeat fully loaded with Cu^{+2} [30].

The two complexes differ greatly in terms of the coordinating ligands, for which a great difference in the λ_{max} associated with these coordination complexes is observed. In this spectrum, solutions of WGQGGGTHNQ and WGQPHGGGWGQPHGGGWGQ were prepared in 10 mM NEM separately and saturated with Cu^{+2} and the CD signal for the complex formed was obtained. The maximum absorption peaks in the visible region of the two complexes differ by about 100 nm. Thus, if the fifth binding site is loaded with Cu^{+2} it can be identified by CD spectrum with λ_{max} of 496 nm and a minimum absorption at 588 nm. Similarly, an octarepeat-Cu^{+2} complex gives a maximum absorption at 588 nm. This data is relevant to individual Cu^{+2} loaded binding units.

Another set of interesting data obtained was the titration curves of the full length Cu^{+2} binding region of PrP (residues 57-98). Figure 4.2 is the spectra of a CD titration performed on

PrP. Various equivalents of Cu^{+2} were titrated into a 100 µM PrP (23-28, 57-98) solution in 10 mM NEM at pH 7.3.

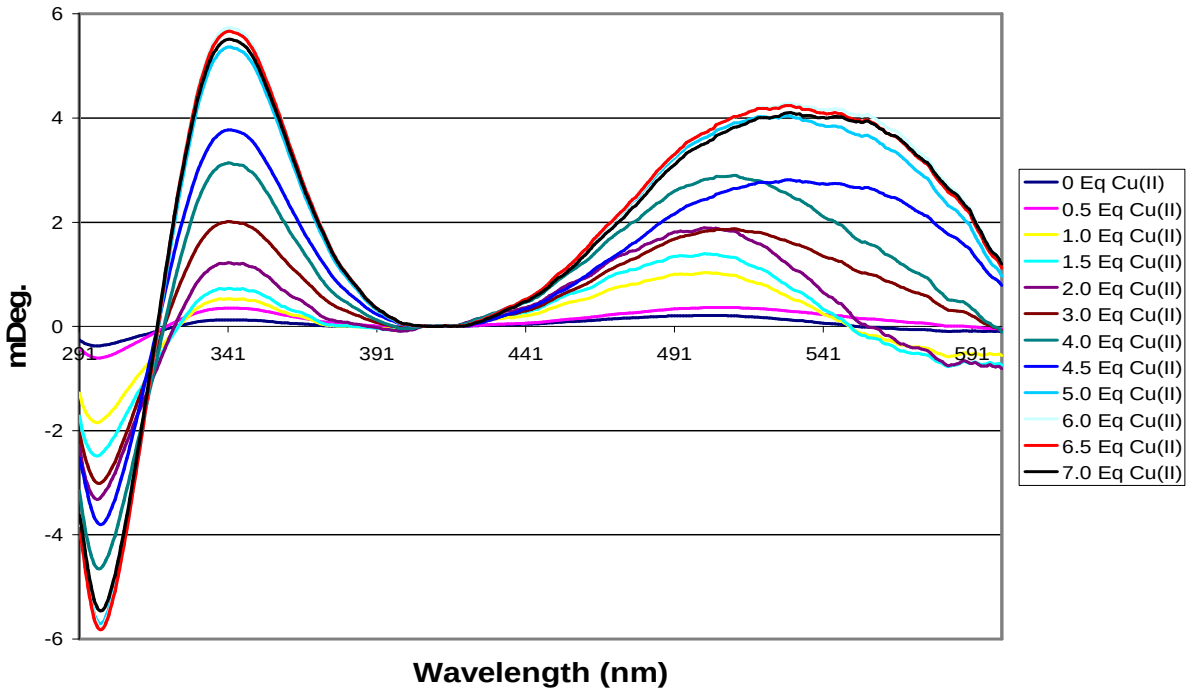

Figure 4.2: Titration of PrP (23-28, 57-98) with Cu^{+2} in NEM buffer[30].

At 0 eq. of Cu^{+2}, where only PrP is present in the solution, no characteristic peaks were observed. On addition of Cu^{+2} peaks appear whose intensity and λ_{max} change consistently with consecutive titration points until a saturation point is reached. Information about the secondary structure of the PrP peptide was not interpreted from these titrations. The peaks in the UV region are due to ligand to metal charge transfer (LMCT) and the peaks in visible region are due to d-d transitions in the Cu^{+2}. In this titration some of the evident peaks in the UV region are a negative peak at 290 nm and a positive band at 345 nm. These peaks can be correlated to amount of Cu^{+2} bound. For the present studies of my project, the area of the interest is the visible region which

gives the idea about the environment of the coordination sphere of the Cu^{+2}. It appears from the figure 4.2 that in the visible region a positive band with a λ_{max} of 500 nm appears at 1 eq. of Cu^{+2} whose intensity increases as more Cu^{+2} is added. After 1.5 eq. of Cu^{+2} a shift to longer wavelength appears. Upon saturation at around 5 Eq of Cu^{+2}, a positive band centered at around 530 nm is seen. From this titration experiment, a conclusion was drawn that the dominant mode of Cu^{+2} binding was different at low Cu^{+2}concentration than at higher concentrations. The shift in the wavelength at higher concentration indicates that there was a change in the coordination sphere of Cu^{+2}. Multivariate Curve Resolution-Alternating Least Squares Analysis was done the titration data. Three pure component spectra were identified in the titration data. Comparing the pure components to the CD data of fragments (as shown in Figure 4.1) revealed specific Cu^{+2} binding structures[30].

From the characteristic signals seen in figure 4.2, it was estimated that the positive band at around 500 nm is comparable to the 498 nm peak of the 5^{th} binding site (figure 4.1). After this binding site is completely saturated on addition of Cu^{+2}, the individual octarepeats start to fill. This is the reason for the shift of the λ_{max} to higher wavelengths as the octarepeats have higher λ_{max} than the 5^{th} binding site when loaded with Cu^{+2}.

To summarize the binding events occurring when Cu^{+2} is titrated into PrP, in each of the 5 binding sites (four octarepeats and fifth binding site) histidine acts as the anchoring site for the copper. Initially, copper coordinates to all or few of the histidines of octarepeats which makes it CD inactive as shown in Figure 1.8 in chapter 1. At intermediate Cu^{2+} occupancy, there is a competition between the multiple histidines and the 5^{th} binding site for Cu^{2+} and the later saturates first followed by the octarepeats.

4.3 Sample Preparation Methodology

The CD titration of Cu^{+2} was done by two different methods which are described in detail in the later part of the section. All the data collected for the Cu^{+2} titrations were on 100 µM of the PrP (23-28, 57-98) in 10 mM ACES. The copper titrated into peptide was prepared from a stock of $CuSO_4$ solution in 10 mM ACES. All solutions were first adjusted to pH of 7.4 using small amounts of known molarity of sodium hydroxide (NaOH) and then made upto the required volume using volumetric flask.

Blank Preparation:

A blank solution of 10 mM ACES was prepared in 18 MΩ cm water from a pre-prepared stock solution of 0.2 M ACES solution.

Peptide Preparation:

The PrP peptide (23-28, 57-98) was synthesized by SPPS, purified and lyophilized. A stock solution of this peptide was prepared in 18 MΩ cm water. The concentration of the stock solution was determined by using ultra-violet visible spectrometry (UV-Vis) in a 1cm quartz cuvette. In the peptide used, 5 tryptophans are present all of which absorb at 280 nm. Trytophan has an extinction coefficient of 5690 M^{-1} cm^{-1}. The exact concentration of the stock solution was determined using Beer-Lambert's Law.

Copper Solution Preparation:

A stock solution of $CuSO_4$ of 15.65 mM concentration was prepared. Various concentrations of the copper solutions required for the titration were prepared from the stock

solution in 10 mM ACES. The pH was adjusted to about 7.4 using 1M NaOH and HCl and the final volume was made up using a volumetric flask.

Optimization of Parameters:

CD experiments were performed on a JASCO J-810 spectophotometer. Two matched quartz cuvettes of 0.1 cm path length were used for blank and sample solutions. The CD instrument is calibrated at regular intervals with a solution of camphor sulfonic acid (CSA). Blank runs are performed at the beginning and end of the titration. Obtaining a good blank signal is very crucial in these titrations as the signal obtained is weak. Blank subtraction is done by the software used in the spectrometer. All the titrations were done at room temperature (20^0C). The sample cuvette used was thoroughly rinsed between runs using methanol, 18 MΩ cm water and 10 mM ACES to ensure that there were no traces of the copper and peptide from the previous sample. The cuvettes are completely dried before use to prevent small but significant dilution effects from the buffer used for rinsing.

CD experiments were performed as discussed in chapter 3 to determine the concentration of the ACES to be used for ITC titrations to keep the peptide at low copper loading state. These experiments were performed from 280 to 800 nm, 4 scans and a bandwidth of 2 nm, a scan speed of 200 nm/min, a data pitch of 0.1 nm and response speed of 1 sec.

As indicated above, the CD titrations were performed using two methods. In the first method, separate solutions of the 100 µM peptide with 1, 2, 5, 10 equivalents of Cu^{+2} were prepared in 10 Mm ACES. Each solution made for the titration was 2.5 ml in volume. The solutions were incubated between 4 and 5 hours to ensure maximal Cu^{+2} loading. For the tiration

involving preparation of these individual complexes of copper PrP, the data pitch was 1 nm to collect fewer data points and number of scans was increased to 8 to get better data.

In the second method, a continuous titration of Cu^{+2} into the 1.4062 mL of 100 µM peptide was performed to reach 5 eq. of Cu^{+2} at the end of the titration. This method of titration was performed to replicate the exact same conditions used in an ITC titration experiment. The table 4.3 below lists the steps, quantities of addition of Cu^{+2} and the molar ratioreached during the titration.

Table 4.1: Calculations for CD titrations

Eq. of Cu^{+2} added	Vol of Cu^{+2} added (mL)	Total vol added (mL)	Vol in Cuvette (mL)	[PrP] (mM)	[Cu^{+2}] (mM)	Molar ratio
0	0	0	1.4062	0.1	0	0
1	0.122	0.122	1.5822	0.092	0.09	1.0
2	0.122	0.244	1.7042	0.086	0.17	2.0
3	0.122	0.366	1.8262	0.079	0.24	3.0
4	0.122	0.488	1.9482	0.075	0.30	4.0
5	0.122	0.610	2.0702	0.070	0.35	5.0

All the calculations shown in table 4.3 are accounted for volume corrections. The dilution of the PrP in the cell due to addition of Cu^{+2} is accounted for in the calculation of the concentration of PrP and Cu^{+2} shown in the table. A 1.2 mM solution $CuSO_4$ was prepared from which 0.122 mL aliquots of Cu^{+2}were added to reach a specific molar ratio of Cu^{+2} / peptide. The waiting time for each addition of Cu^{+2} added is around half an hour with vigorous shaking on a

vortex. For these titrations the number of scans was increased to 16 and band width parameter was optimized to 4 nm based on experimental data shown in figure 4.3. The other parameters were the same as the previous titration method.

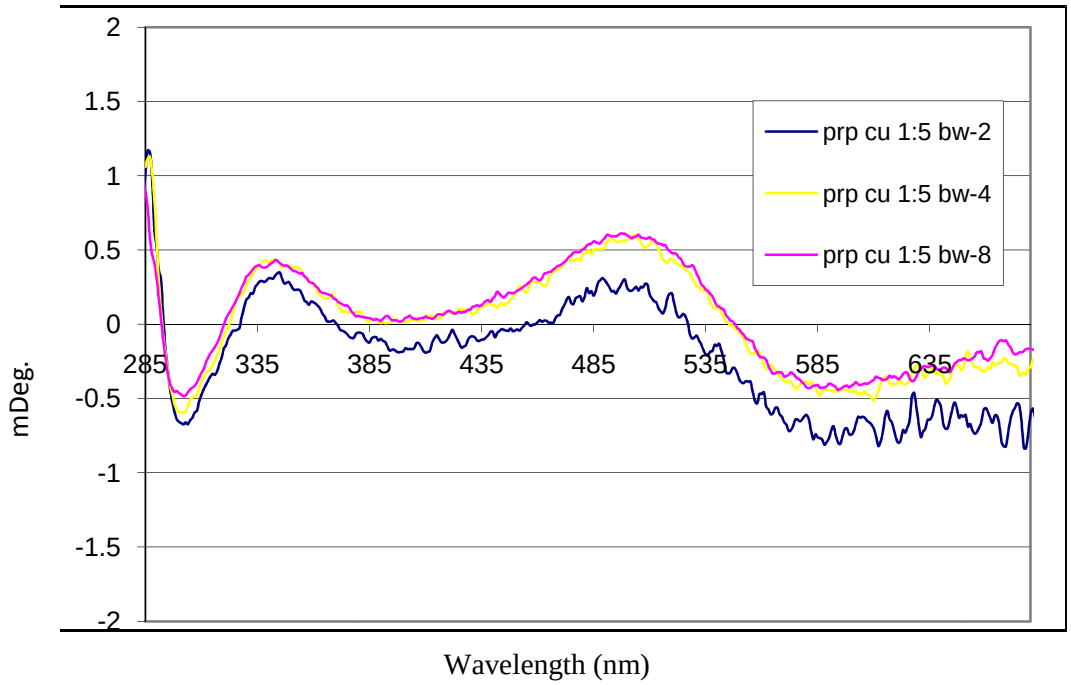

Figure 4.3: CD signal of PrP(23-28, 57-98) as a function of bandwidth.

Another important component of the CD spectrum is High Tension (HT) voltage which is a measure of the applied voltage to the detector. In case of low intensity signals in CD, the detector increases the voltage to increase the sensitivity. If a value of 400 volts on the detector has been reached or if the voltage rises rapidly, the CD signal becomes unreliable as the signal might not accurately represent the light absorbed by the sample.

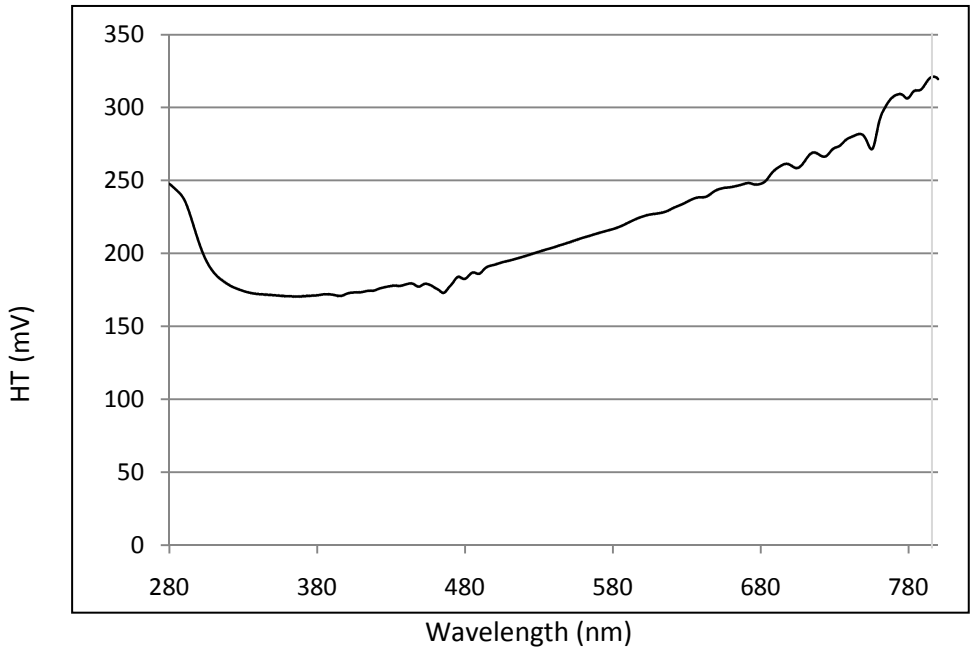

Figure 4.4: HT signal for the 5:1 complex of PrP in 10 mM ACES

The figure given above is the example of the HT signal data for one of the runs on CD and the HT signal for all the CD runs are quite similar to the one shown here. From the graph it is clear that the HT is stable between 400 nm to 680 nm and data obtained outside this range is unreliable.

4.4 Titration of Copper into Native PrP (23-28, 57-98)

As discussed earlier native PrP (57-98) is the main copper binding region of the protein and has 4 repeats of the octarepeat region PHGGGWGQ and the GGGTH site for copper coordination. It binds up to 5 coppers at a pH of 7.4 involving the histidines and the amide bonds of the nearby peptide backbone.

In the first method of titration as described in earlier chapter, individual solutions of various eq. of Cu^{+2} were prepared. The absorption of these solutions was monitored by using CD. Figure 4.5 shows the spectrum obtained.

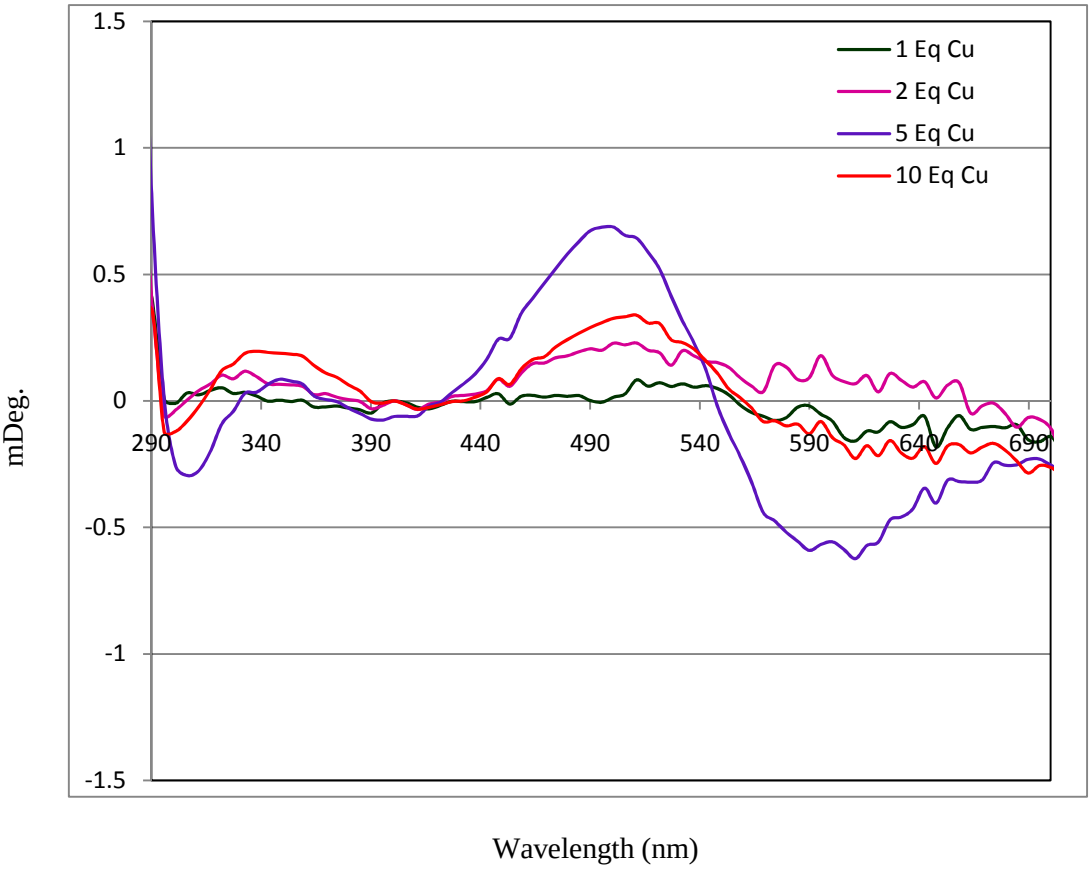

Figure 4.5: CD spectrum of titration of 100 µM PrP(23-28,57-98) with Cu^{+2} (10 mM ACES).

In the CD spectrum collected, the signal obtained is very weak because of the different buffer (ACES) used when compare to previous studies done in NEM buffer. ACES is a highly competing buffer when compared to NEM. So, the population of copper bound PrP is comparatively less and so the intensity of the signal is less. Experiments done to determine this have already been discussed in chapter 3.The negative band at 290 nm and the positive band at 340 nm are due to LMCT and were exactly same in the CD titration observed before expect for the intensity difference. At 1 eq. of Cu^{+2} a baseline is seen as the first mode of binding in PrP is CD inactive. As the eq. of copper increase to 5 eq. a positive band appears in the visible region at 500 nm which indicates Cu^{+2} coordinating to the histidine of the 5^{th} binding site. At 10 Eq. of Cu^{+2} the intensity seems to have been decreased. This could possibly be the beginning of loading of the individual octarepeats with Cu^{+2}. In the visible region, until 5 Eq of Cu^{+2} all the positive bands are centered at 500 nm. As the data becomes very noisy after 590 nm, no conclusions were derived from this part of the graph.

4.5 Native PrP Titration Data

To complement the data from the ITC titrations CD experiments were designed for titrating 1, 2, 3, 4, 5 equivalents of copper into PrP peptide. The titration conditions were exactly same as the ITC. This was done to have an estimate of the number of Eq. of Cu^{+2} bound to PrP by the end of the titration and also compare the type of Cu^{+2} coordination that occurs in this system when compared to the earlier titrations discussed in chapter 4.2. So, through this titration we could confirm the low copper loading state of the peptide and also the stoichiometry of the copper PrP binding. This information will aid in for ITC data analysis. In these experiments we focused only on the d-d transitions of the Cu^{+2} in the visible region.

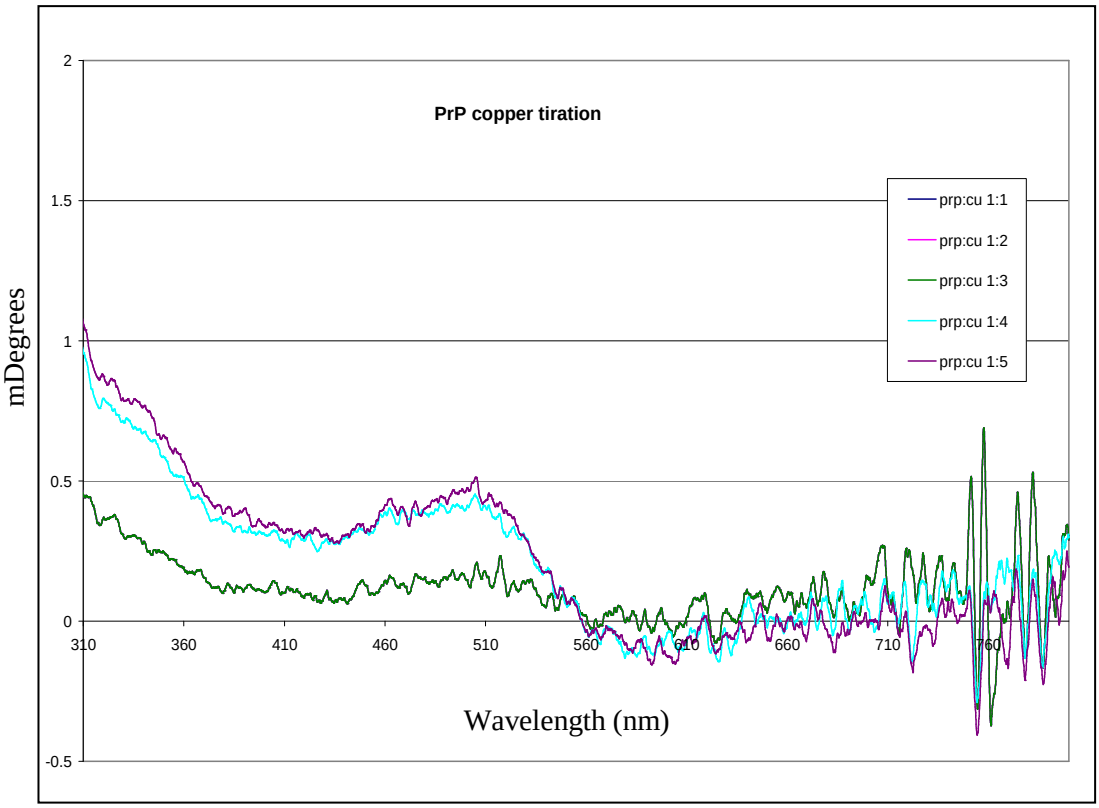

Figure 4.6: Tiration of the native PrP peptide with Cu^{+2}(10 mM ACES).

As the parameters were optimized the noise was reduced when compared to CD data in figure 4.5. The unsmoothed CD spectrum obtained from titration of Cu^{+2} into the native PrP is shown in figure 4.6. Previous CD data showed a λ_{max} of 590 nm for HGGGW Cu^{+2} coordination sphere and a λ_{max} of 500 nm and a minima of 590 nm for GGGTH Cu^{+2} coordination sphere when the peptide is fully copper loaded. Based on this information some conclusions could be made. It is evident from the CD data that at 1, 2, 3 eq. of Cu^{+2} titration into the native PrP there is very little signal and they overlap over each other. Initially, a positive band roughly appears at 500 nm. As more Cu^{+2} is titrated into the solution an increase in intensity of signal is found but no shift in wavelength is observed as expected. At 5 eq. of Cu^{+2} the system appears to be saturated. We hypothesize that only 2:1 molar ratio of copper: prion complex is attained by the end of the titration. The 1:1 complex of copper prion is CD inactive and hence not visible in the titration and the 2:1 complex produces a CD spectrum with a positive band at approximately 500 nm. This wavelength is characteristic for the 5^{th} binding site, GGGTH. Further, individual octrapeat binding doesn't occur as no shift of the λ_{max} occurs which is characteristic for the HGGGGW-Cu^{+2} complex. Based on all these observations it appears that even at 5 Eq of Cu^{+2} only a 2: 1 complex is formed. Thus, confirming that the ITC studies are done at low copper loading state as per the research goal.

Chapter 5: Data Analysis and Conclusions

5.1 ITC Data Analysis

ITC data analysis is done by fitting the titration data with an appropriate model to obtain the thermodynamic parameters. Several software formats are available to fit the ITC data. The software used for the purpose of fitting the data was Origin™. The three common fitting models used are 'one set of sites', 'two set of sites' and 'sequential binding sites'. In the first case, the system is assumed to have n binding sites of equal affinity and in the second case the system is assumed to have n_1 binding sites of a particular affinity and n_2 binding sites with a different affinity. Lastly, the sequential binding sites model assumes n sites each with a different affinity.

Binding models used for 'two sets of sites' and 'sequential binding sites':

Forward Titration:

Cell : PrP

Syringe: Cu

$$PrP + Cu \overset{K_1}{\rightleftharpoons} PrP\text{-}Cu$$

$$PrP\text{-}Cu + Cu \overset{K_2}{\rightleftharpoons} PrP\text{-}Cu_2$$

$$K_1 = \frac{[PrP\text{-}Cu]}{[PrP][Cu]}$$

$$K_2 = \frac{[PrP\text{-}Cu_2]}{[PrP\text{-}Cu][Cu]}$$

Reverse titration:

Cell : Cu

Syringe: PrP

$$PrP + 2Cu \underset{}{\overset{K_1^1}{\rightleftharpoons}} PrP\text{-}Cu_2$$

$$PrP\text{-}Cu_2 + PrP \underset{}{\overset{K_2^1}{\rightleftharpoons}} 2PrP\text{-}Cu$$

$$K_1^1 = \frac{[PrP\text{-}Cu_2]}{[PrP]\,[Cu]^2}$$

$$K_2^1 = \frac{[PrP\text{-}Cu]^2}{[PrP\text{-}Cu_2][PrP]}$$

$\boldsymbol{\beta = K_1 \times K_2 = K_1'}$

$\boldsymbol{K_1' = K_1 \times K_2}$

$\boldsymbol{\Delta H_1' = \Delta H_1 + \Delta H_2}$

All the fitting models evaluate the change in the heat content, $\Delta Q_{(i)}$ from completion of the $i^{th} - 1$ injection to completion of the i^{th} injection for a solution contained in the volume V_0 . Different models have different $\Delta Q_{(i)}$ values based on the binding in consideration.

$$\Delta Q_{(i)} = Q_{(i)} + \frac{dV_i}{V_o}\left[\frac{Q_{(i)} - Q_{(i-1)}}{2}\right] - Q_{(i-1)}$$

$\Delta Q_{(i)}$ - heat content for the i^{th} injection

$\Delta Q_{(i-1)}$ - heat content for the i^{th}-1injection

V_0 - standard active cell volume which is unique to the brand of calorimeter

The second term in the above equation is for the displaced volume upon injection of the titration.

While fitting a model to the ITC data, an initial guess for all the values of n, K and ΔH is made. Calculation of $\Delta Q_{(i)}$ is done for each injection and compared to the experimental fit values. The fit parameters are then improved by using a standard Marquadt algorithm. This procedure is iterated until Chi^2 no longer minimizes. Once the final values of n, K and ΔH are obtained the ΔS value is calculated.

Fitting of the ITC data was done on the concatenated forward and reverse titrations. In the case of the reverse titration since the ligand is in the cell and not in the syringe, this is taken into consideration during the fitting. Hence, fitting the data with a correct model should return the same thermodynamic parameters for both forward and reverse titration. All the fitting was done after removing the first data point and any bad data points due to concatenation of the runs.

We started the data fitting with the simplest model, the 'one set of sites' model. Analyzing the data with this model gave unrealistic n value of less than 0.01and chi^2 couldn't be reduced.

Using the 'two set of sites' model gave a better fit when compared to the one set of sites model but the values of the thermodynamic parameters for the two sites were not reproducible for the three runs especially the n values and the error values from the Origin software were very high.

Since, ΔH is indicative of the total heat involved in the reaction which is the difference in heats between the initial and completion points of the binding event, an average ΔH value was

calculated from 3 most reproducible runs (initial runs with 0.09 mM Cu^{+2} into 0.07 mM PrP) as the single injection runs were not successful. The ΔH (apparent) value for the initial event is -2.4×10^3 kcal/mole with standard error of 0.1 kcal/mole.

The apparent ΔH value includes the following equilibria:

$$Cu\ ACES \rightleftharpoons Cu + ACES$$

$$PrPH \rightleftharpoons PrP + H^+$$

$$Cu + PrP \rightleftharpoons Cu\ PrP$$

$$H^+ + ACES \rightleftharpoons ACESH$$

This value was considered as ΔH_1 and fixed in the data fitting process to aid in the fitting of the parameters but didn't reduce the errors.

Finally, the sequential model with n = 2 was adopted. As the CD titration data that complemented the ITC data showed the binding of two coppers, we hypothesize that by the end of the ITC titration in 10 mM ACES only 2 binding events occur. Fitting the sequential binding model to the forward and reverse titration didn't provide a good fit to the data. The forward titration was not buffer subtracted as the value of heat of dilution is very close to zero but the reverse titration was buffer subtracted.

Table 5.1: Thermodynamic parameters obtained from forward titration by fitting a sequential binding model.

Thermodynamic Parameters	**Run 1**	**Run2**	**Run 3**
K_1	1.84 (± 0.22) x 10^4	1.48 (± 0.19) x 10^4	1.82 (± 0.31) x 10^4
K_2	202 (± 33)	139 (± 16)	121 (± 21)
ΔH_1 (cal/mol)	-3509 (± 162)	-4074 (± 218)	-3192 (± 204)
ΔH_2 (cal/mol)	-1.654 (± 0.37) x 10^4	-4.276 (± 0.62) x 10^4	-5.242 (± 0.10) x 10^4
ΔS_1 (cal/mol K)	7.75	5.42	8.79
ΔS_2 (cal/mol K)	-44.9	-134	-166

Table 5.2: Thermodynamic parameters obtained from reverse titration by fitting a sequential binding model.

Thermodynamic Parameters	**Run 1**	**Run2**
K_1	1.25 (± 0.11) x 10^3	1.31 (± 0.11) x 10^4
K_2	1.07 (± 0.09) x 10^4	1.54 (± 0.13) x 10^3
ΔH_1 (cal/mol)	-4509 (± 1040)	-6771 (± 120)
ΔH_2 (cal/mol)	-4.053 (± 0.397) x 10^4	-4894 (± 191)
ΔS_1(cal/mol K)	-0.948	-3.87
ΔS_2(cal/mol K)	-177	-1.84

From the above tables, it can be observed the thermodynamic parameters are not reproducible in both forward and reverse titration. From the (forward titration) thermodynamic parameter values it is evident that K_1 is greater than K_2 indicating stronger binding for the first event. It also tells us that the second binding event is more exothermic than the first one. For the first event since ΔH_1 is negative and ΔS_1 is positive the reaction is favorable. In the case of second binding event, negative ΔS_2 probably indicates more order in the system in relative to the first event. A trend can be hypothesized from the thermodynamic data for the forward titration. The first binding event is both entropically and enthalpically favored whereas the second binding event is only enthalpically favored. On the contrary, the first run of the reverse titration shows that K_2 is greater than K_1 which is not consistent with the results from the forward titration. Moreover, the K values in the reverse titration differ by an order of magnitude between the two runs.

It was observed the initial part of the titration curve didn't have the appropriate fitting as the later part of the curve as shown in the diagram 5.1.

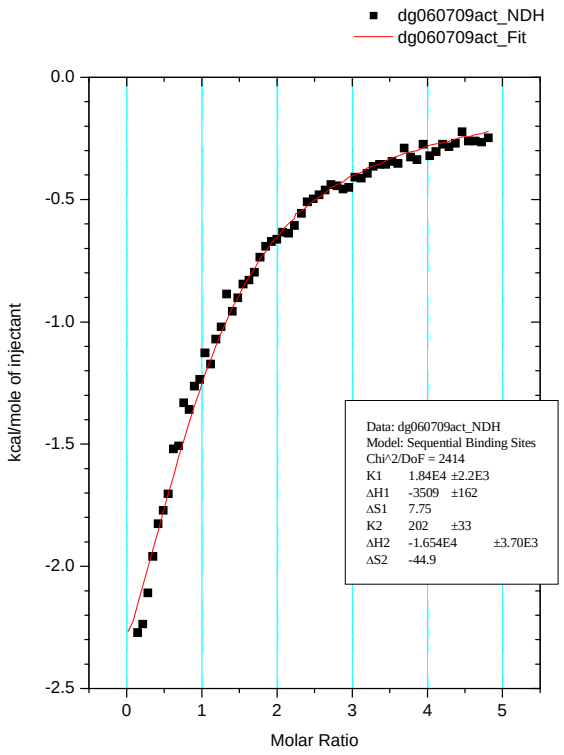

Figure 5.1: Representative ITC data for the forward titration of Cu^{+2} into PrP (23-28, 57-98) fitted using the sequential binding sites model with n = 2. The best fit parameters are shown at the bottom right.

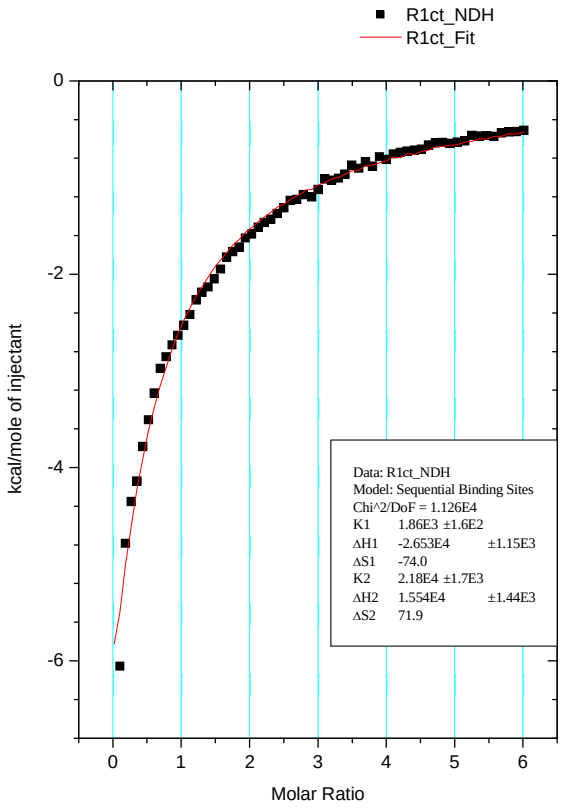

Figure 5.2: Representative ITC data for the reverse titration of Cu^{+2} into PrP (23-28, 57-98) fitted using the sequential binding sites model with n = 2. The best fit parameters are shown at the bottom right.

In order to improve the fitting parameters we hypothesiszed a new binding model which may account for the subtle inflection observed at the molar ratio of 0.5 Cu^{+2}: PrP. Before the 1:1 complex is formed there is a probable existence of another early event at around 0.5:1 of copper to PrP. This involves the cross linking of two PrP's by a single copper. This idea has been suggested before through experiments done on BoPrP discussed in the introduction chapter as shown in the figure 5.3.

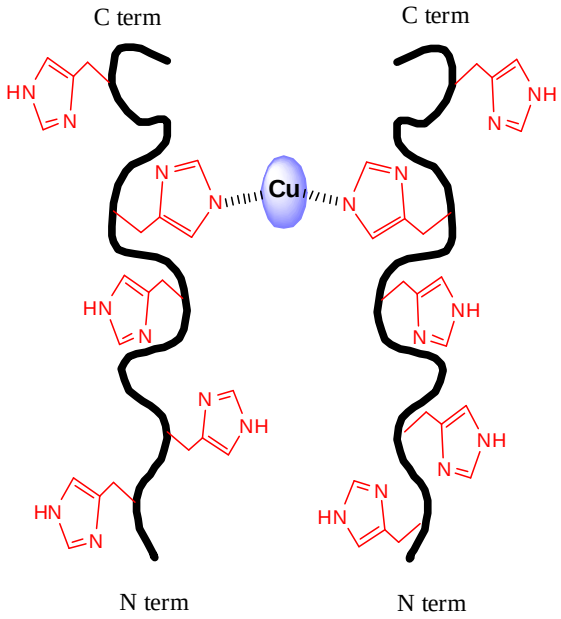

Figure 5.3: PrP cross- linking by a single copper ion.

New hypothesized binding model:

	Cu: PrP
2PrP + 1Cu-----> PrP_2-Cu	**0.5: 1**
PrP_2-Cu + 1Cu----> 2 PrP-Cu	**1: 1**
2PrP-Cu +2Cu----> 2 Prp-Cu_2	**2: 1**

The ITC fitting program needs to be modified in order to fit this binding model and this work is currently in progress.

In conclusion, from the CD data we conclude that the PrP peptide (57-98) binds only 2 coppers in 10 mM ACES buffer. Fitting the ITC data with the existing models, i.e one sets of sites, two sets of sites or sequential binding, lead to unsatisfactory fits suggesting a more complex binding process. The hypothesized model above will hopefully lead to good fits of the

ITC data and will support the hypothesis that Cu^{+2} is cross- linking PrP molecules at low equivalents of added Cu^{+2} .

REFERENCES

1. Prusiner, S. B. (1997). Prion diseases and the BSE crisis. *Science (New York, N.Y.), 278*(5336), 245-251.

2. Prusiner, S. (1982). Novel proteinaceous infectious particles cause scrapie. *Science, 216*(4542), 136-144.

3. Prusiner, S. B. (1998). Prions. *Proceedings of the National Academy of Sciences of the* United *States of America,* 95(23), 13363-13383.

4. Riek, R., Hornemann, S., Wider, G., Glockshuber, R., & Wuthrich, K. (1997). NMR characterization of the full-length recombinant murine prion protein, mPrP(23-231). *FEBS Letters, 413*(2), 282-288.

5. Donne, D. G., Viles, J. H., Groth, D., Mehlhorn, I., James, T. L., Cohen, F. E., et al. (1997). Structure of the recombinant full-length hamster prion protein PrP(29-231): The N terminus is highly flexible. *Proceedings of the National Academy of Sciences of the United States of America, 94*(25), 13452-13457.

6. Zahn, R., Liu, A., Luhrs, T., Riek, R., von Schroetter, C., Lopez Garcia, F., et al. (2000). NMR solution structure of the human prion protein. *Proceedings of the National Academy of Sciences of the United States of America, 97*(1), 145-150.

7. Lopez Garcia, F., Zahn, R., Riek, R., & Wuthrich, K. (2000). NMR structure of the bovine prion protein. *Proceedings of the National Academy of Sciences of the United States of America, 97*(15), 8334-8339.

8. Uversky, V. N., Gillespie, J. R., & Fink, A. L. (2000). Why are "natively unfolded" proteins unstructured under physiologic conditions? *Proteins, 41*(3), 415-427.

9. Bueler, ,Hansruedi, Fischer, ,Marek, Lang, ,Yolande, Bluethmann, ,Horst, Lipp, ,Hans-Peter, DeArmond, S.,J., et al. Normal development and behaviour of mice lacking the neuronal cell-surface PrP protein.

10. Brown, D. R., Qin, K., Herms, J. W., Madlung, A., Manson, J., Strome, R., et al. (1997). The cellular prion protein binds copper in vivo. *Nature, 390*(6661), 684-687.

11. Chesebro, B. (1999). Prion protein and the transmissible spongiform encephalopathy diseases. *Neuron, 24*(3), 503-506.

12. Pauly, P. C., & Harris, D. A. (1998). Copper stimulates endocytosis of the prion protein. *The Journal of Biological Chemistry, 273*(50), 33107-33110.

13. Brown, L. R., & Harris, D. A. (2003). Copper and zinc cause delivery of the prion protein from the plasma membrane to a subset of early endosomes and the golgi. *Journal of Neurochemistry, 87*(2), 353-363.

14. Brown, D. R., Wong, B. S., Hafiz, F., Clive, C., Haswell, S. J., & Jones, I. M. (1999). Normal prion protein has an activity like that of superoxide dismutase. *The Biochemical Journal, 344 Pt 1*, 1-5.

15. Wopfner, F., Weidenhofer, G., Schneider, R., von Brunn, A., Gilch, S., Schwarz, T. F., et al. (1999). Analysis of 27 mammalian and 9 avian PrPs reveals high conservation of flexible regions of the prion protein. *Journal of Molecular Biology, 289*(5), 1163-1178.

16. Bocharova, O. V., Breydo, L., Salnikov, V. V., & Baskakov, I. V. (2005; 2005). Copper (II) inhibits in vitro conversion of prion protein into amyloid fibrilsâ€ . *Biochemistry, 44*(18), 6776-6787.

17. Hornshaw, M. P., McDermott, J. R., & Candy, J. M. (1995). Copper binding to the N-terminal tandem repeat regions of mammalian and avian prion protein. *Biochemical and Biophysical Research Communications, 207*(2), 621-629.

18. Hornshaw, M. P., McDermott, J. R., Candy, J. M., & Lakey, J. H. (1995). Copper binding to the N-terminal tandem repeat region of mammalian and avian prion protein: Structural studies using synthetic peptides. *Biochemical and Biophysical Research Communications, 214*(3), 993-999.

19. Whittal, R. M., Ball, H. L., Cohen, F. E., Burlingame, A. L., Prusiner, S. B., & Baldwin, M. A. (2000). Copper binding to octarepeat peptides of the prion protein monitored by mass spectrometry. *Protein Science: A Publication of the Protein Society, 9*(2), 332-343. 9.2.332

20. Vassallo, N., & Herms, J. (2003). Cellular prion protein function in copper homeostasis and redox signalling at the synapse. *Journal of Neurochemistry, 86*(3), 538-544.

21. Miura, T., Hori-i, A., Mototani, H., & Takeuchi, H. (1999). Raman spectroscopic study on the copper(II) binding mode of prion octapeptide and its pH dependence. *Biochemistry, 38*(35), 11560-11569.

22. Aronoff-Spencer, E., Burns, C. S., Avdievich, N. I., Gerfen, G. J., Peisach, J., Antholine, W. E., et al. (2000). Identification of the Cu2+ binding sites in the N-terminal domain of the prion protein by EPR and CD spectroscopy. *Biochemistry, 39*(45), 13760-13771.

23. Burns, C. S., Aronoff-Spencer, E., Dunham, C. M., Lario, P., Avdievich, N. I., Antholine, W. E., et al. (2002). Molecular features of the copper binding sites in the octarepeat domain of the prion protein. *Biochemistry, 41*(12), 3991-4001.

24. Burns, C. S., Aronoff-Spencer, E., Legname, G., Prusiner, S. B., Antholine, W. E., Gerfen, G. J., et al. (2003). Copper coordination in the full-length, recombinant prion protein. *Biochemistry, 42*(22), 6794-6803.

25. Jones, C. E., Klewpatinond, M., Abdelraheim, S. R., Brown, D. R., & Viles, J. H. (2005). Probing copper2+ binding to the prion protein using diamagnetic nickel2+ and 1H NMR: The unstructured N terminus facilitates the coordination of six copper2+ ions at physiological concentrations. *Journal of Molecular Biology, 346*(5), 1393-1407.

26. Chattopadhyay, M., Walter, E. D., Newell, D. J., Jackson, P. J., Aronoff-Spencer, E., Peisach, J., et al. (2005; 2005). The octarepeat domain of the prion protein binds cu(II) with three distinct coordination modes at pH 7.4. *Journal of the American Chemical Society, 127*(36), 12647-12656.

27. Walter, E. D., Chattopadhyay, M., & Millhauser, G. L. (2006). The affinity of copper binding to the prion protein octarepeat domain: Evidence for negative cooperativity. *Biochemistry, 45*(43), 13083-13092.

28. Gonzalez-Iglesias, R., Elvira, G., Rodriguez-Navarro, J. A., Velez, M., Calero, M., Pajares, M. A., et al. (2004). Cu2+ binding triggers alphaBoPrP assembly into insoluble laminar polymers. *FEBS Letters, 556*(1-3), 161-166.

29. Morante, S., Gonzalez-Iglesias, R., Potrich, C., Meneghini, C., Meyer-Klaucke, W., Menestrina, G., et al. (2004). Inter- and intra-octarepeat cu(II) site geometries in the prion protein: Implications in cu(II) binding cooperativity and cu(II)-mediated assemblies. *The Journal of Biological Chemistry, 279*(12), 11753-11759.

30. Pollock, J. B., Cutler, P. J., Kenney, J. M., Gemperline, P. J., & Burns, C. S. (2008). Characterization of Cu2+-binding modes in the prion protein by visible circular dichroism and multivariate curve resolution. *Analytical Biochemistry, 377*(2), 223-233.

31. Kenward, A. G., Bartolotti, L. J., & Burns, C. S. (2007; 2007). Copper and zinc promote interactions between membrane-anchored peptides of the metal binding domain of the prion proteinâ€ . *Biochemistry, 46*(14), 4261-4271.

32. Lance, E. A., Rhodes, C. W.,3rd, & Nakon, R. (1983). Free metal ion depletion by "good's" buffers. III. N-(2-acetamido)iminodiacetic acid, 2:1 complexes with zinc(II), cobalt(II),

nickel(II), and copper(II); amide deprotonation by zn(II), co(II), and cu(II). *Analytical Biochemistry, 133*(2), 492-501.

33. Pierce, M. M., Raman, C. S., & Nall, B. T. (1999). Isothermal titration calorimetry of Protein–Protein interactions. *Methods, 19*(2), 213-221.

34. ITC Data Analysis in Origin, Manual Version 7.0, January 2004, Accessed 2008.